Biomagnetism

8

The field of *biomagnetism* has exploded in recent decades. Magnetic signals have been detected from the heart, brain, skeletal muscles, and isolated nerve and muscle preparations. Measurements of the magnetic susceptibility of the lung show the effect of dust inhalation. Susceptibility measurements of the heart can determine blood volume, while the susceptibility of the liver can measure iron stores in the body. Bacteria and some animals contain aggregates of magnetic particles, often attached to neural tissue. Bacteria use these magnetic particles to determine which way is down. Magnetism is used for orientation by birds and other animals.

Sections 8.1 and 8.2 review the basics of magnetism. Section 8.3 calculates the magnetic field of an axon in an infinite conducting medium. This result, which shows that the field is due primarily to the current dipole in the interior of the axon, is approximately true for the magnetocardiogram and evoked responses from the brain, described in Sects. 8.4 and 8.5.

Section 8.6 reviews electromagnetic induction. Section 8.7 describes the use of varying magnetic fields to stimulate nerves or muscles. Section 8.8 introduces diamagnetic, paramagnetic, and ferromagnetic materials and describes biomagnetic effects that depend on magnetic materials. Section 8.9 reviews instrumentation for measuring these weak magnetic signals.

8.1 The Magnetic Force on a Moving Charge

Lodestone, compass needles, and other forms of magnetism have been known for centuries, but it was not until 1820 that Hans Christen Oersted showed that an electric current could deflect a compass needle. We now know that magnetism results from electric forces that moving charges exert on other moving charges and that the appearance of the magnetic force is a consequence of special relativity. An excellent development of magnetism from this perspective is found in Purcell and Morin (2013). The development here is more traditional (Griffiths 2013) and is incomplete.

Suppose that a beam of electrons is accelerated in a cathode-ray tube (as in an oscilloscope, computer display, or television receiver) and causes a spot of light to be emitted where it strikes a fluorescent screen. The electron source is cathode C in Fig. 8.1. The accelerating electrode is E. The fact that the beam is accelerated toward a positively charged electrode confirms that the electrons are negatively charged. The beam normally strikes the screen at point X. Placing a battery between plates A and B creates an electric field that deflects the beam as it passes between the plates. If plate A is positively charged, the beam is deflected upward to point Y. If the battery is removed and the north pole of a bar magnet is brought to the position shown, the beam is deflected to point Z.

We say that a *magnetic field* exists in the space surrounding the bar magnet and that the direction of the magnetic field at any point is the direction a small compass needle located there would point. Experiments show that the force is at right angles to both the direction of the magnetic field and the velocity of the charged particle, and that the magnitude of the force $\mathbf{F}$ is proportional to the charge, the magnitude of the velocity $\mathbf{v}$, and the strength of magnetic field $\mathbf{B}$. (In fact, modern definitions of the magnetic field are based on this proportionality.) The magnitude of the force is greatest when $\mathbf{v}$ and $\mathbf{B}$ are perpendicular. We have seen a relationship like this between three vectors before: the vector product or cross product, which was associated with torque and defined in Sect. 1.5. We write

$$\mathbf{F} = q(\mathbf{v} \times \mathbf{B}). \tag{8.1}$$

The SI unit of $\mathbf{B}$ is the tesla, T. An earlier name was the weber per square meter. Another unit is the gauss, G: $1\ \mathrm{T} = 10^4\ \mathrm{G}$.

8.1.1 The Lorentz Force

If a coordinate system is set up so that $\mathbf{v}$ is along the x axis and $\mathbf{B}$ is along the y axis, then $\mathbf{v} \times \mathbf{B}$ and the force

R. K. Hobbie, B. J. Roth, *Intermediate Physics for Medicine and Biology*,
DOI 10.1007/978-3-319-12682-1_8,

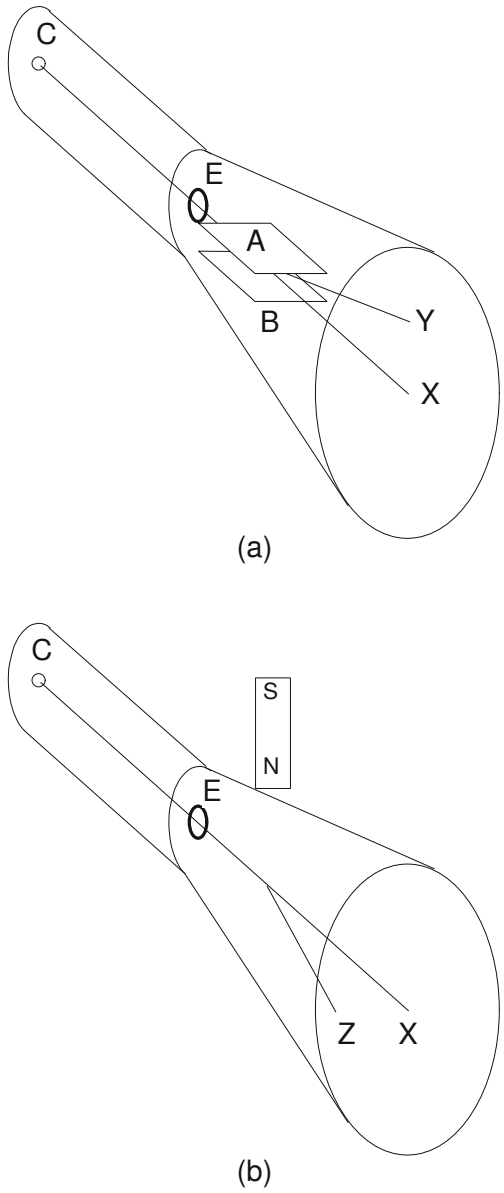

Fig. 8.1 An electron beam generated at cathode C and accelerated through electrode E strikes the fluorescent screen on the *right*. **a** A positive charge on plate A and negative charge on plate B deflects the beam from X to Y. **b** A bar magnet brought close as shown deflects the beam to point Z

on a positive charge are along the $+z$ axis. For negatively charged electrons $\mathbf{F}$ is in the opposite direction. Combining Eq ref8.01 with the electric force gives the full expression for the electromagnetic force, often called the *Lorentz force*:

$$\mathbf{F} = q(\mathbf{E} + \mathbf{v} \times \mathbf{B}). \tag{8.2}$$

Since current in a wire is the result of moving charges, there is a force on a segment of wire carrying a current. Suppose that there are C particles per unit volume, each with charge q, drifting with speed v along a segment of wire of length ds and cross sectional area S. In time dt the total

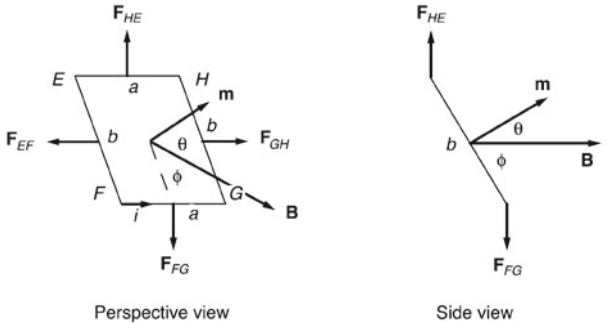

Fig. 8.2 A current-carrying loop is in a uniform magnetic field. The *dashed line* from the *center* of the loop to the *center* of edge FG, vector $\mathbf{B}$ and vector $\mathbf{m}$ all lie in the same plane. The sum of angles θ and ϕ is $\pi/2$. The forces on opposite sides add to zero. There is a torque on the loop unless its plane is perpendicular to the field ($\phi = \pi/2$). The magnetic moment $\mathbf{m}$ is perpendicular to the plane of the loop

charge passing a given plane is $CvqS\,dt$ (see Eq. 4.11) so that the current is $i = CvqS$. If there is a magnetic field perpendicular to the wire, the magnitude of the force on each particle is qvB and the total force is $CS\,ds\,qvB = iB\,ds$. If vector $d\mathbf{s}$ is defined along the wire in the direction of the positive current, then the contribution to the magnetic force from this segment of the wire is

$$d\mathbf{F} = i(d\mathbf{s} \times \mathbf{B}). \tag{8.3}$$

If a small rectangular loop of wire is placed in a uniform magnetic field and a current is made to flow in the wire, there is a magnetic force on each arm of the loop. (The current can be led to and from the rectangle by two parallel closely spaced wires, in which the forces cancel because the currents are in opposite directions. Forces not considered here maintain the position of the loop.) Figure 8.2 shows the orientation of the loop in the horizontal magnetic field. The magnetic moment $\mathbf{m}$ is perpendicular to the loop and makes an angle θ with the direction of $\mathbf{B}$. Sides HE and FG are of length a and perpendicular to the field. The other two sides have length b. The force on side EF has magnitude $iBb\sin\phi$ and is directed as shown. Side GH has a force of equal magnitude in the opposite direction. On side FG the force is down and on side HE it is up, both with magnitude iBa. The vector sum of all the forces is zero. There is a torque, however. If the torque is taken about the center of the loop, the FG force and HE force each exert a torque of magnitude $(iBa)(b/2)\cos\phi$. The total torque is therefore $iBab\cos\phi$. The loop is said to have a magnetic moment $\mathbf{m}$ of magnitude iS, where $S = ab$ is the area of the loop. Vector $\mathbf{m}$ is defined to point perpendicular to the loop in the direction of the thumb of the right hand when the fingers curl in the direction of the current around the loop. The units of $\mathbf{m}$ are A m^2 or J T^{-1}. In terms of angle θ between $\mathbf{m}$ and $\mathbf{B}$, the torque $\boldsymbol{\tau}$ exerted by the magnetic field on the magnetic moment has

magnitude $iabB\sin\theta$, so

$$\boldsymbol{\tau} = \mathbf{m} \times \mathbf{B}. \tag{8.4}$$

The torque is zero when **m** and **B** are parallel or antiparallel. When they are parallel the equilibrium is stable: if there is a small rotation of **m** the torque acts to return it to equilibrium. When they are antiparallel, the equilibrium is unstable.

A small current loop can be used to test for the presence of a magnetic field. At equilibrium **m** points in the same direction that a small compass needle would point and gives the direction of **B**. Measuring the torque for a known displacement of **m** from this direction gives the magnitude of **B**.

8.1.2 The Cyclotron

One important application of magnetic forces in medicine is the *cyclotron*. Many hospitals have a cyclotron for the production of radiopharmaceuticals, especially for the generating positron-emitting nuclei for use in *Positron Emission Tomography (PET)* imaging (see Chap. 17).

Consider a particle of charge q and mass m, moving with speed v in a direction perpendicular to a magnetic field **B**. The magnetic force will bend the path of the particle into a circle. Newton's second law states that the mass times the centripetal acceleration, v^2/r, is equal to the magnetic force

$$mv^2/r = qvB. \tag{8.5}$$

The speed is equal to circumference of the circle, $2\pi r$, divided by the period of the orbit, T. Substituting this expression for v into Eq. (8.5) and simplifying, we find

$$T = 2\pi m/(qB). \tag{8.6}$$

In a cyclotron particles orbit at the *cyclotron frequency*, $f = 1/T$. Because the magnetic force is perpendicular to the motion, it does not increase the particles' speed or energy. To do that, the particles are subjected periodically to an electric field that changes direction with the cyclotron frequency so that it is always accelerating, not decelerating the particles. This would be difficult if not for the fortuitous disappearance of both v and r from Eq. (8.6), so that the cyclotron frequency only depends on the charge-to-mass ratio of the particles and the magnetic field, but not on their energy.

Typically, protons are accelerated in a magnetic field of about 1 T, resulting in a cyclotron frequency of approximately 15 MHz. Each orbit raises the potential of the proton by about 100 kV. It must circulate enough times to raise its total energy to at least 10 MeV so that it can overcome the electrostatic repulsion of the target nucleus and cause nuclear reactions. For example, the high-energy protons may be incident on a target of ^{18}O (a rare but stable isotope of oxygen), initiating a nuclear reaction that results in the production of ^{18}F, an important positron emitter used in PET studies.

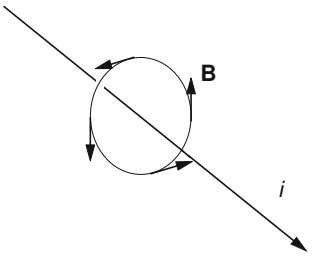

Fig. 8.3 The magnetic field around a current-carrying wire is at right angles to the wire and the perpendicular from the observation point to the wire. The magnitude is inversely proportional to the distance from the wire

8.2 The Magnetic Field of a Moving Charge or a Current

8.2.1 The Divergence of the Magnetic Field is Zero

With a compass needle or small sensing coil we can in principle map the magnetic field surrounding a bar magnet or a wire carrying a current. If we examine the field near a long straight wire carrying current i, we find that **B** is always at right angles to the wire and at distance r has magnitude

$$B = \frac{\mu_0 i}{2\pi r}. \tag{8.7}$$

The constant μ_0 is analogous to ϵ_0 in electrostatics and is $4\pi\times10^{-7}$ T m A^{-1} (or Ω s m^{-1}). Figure 8.3 shows the direction of **B** at various locations around a wire. The direction of the force is consistent with Eq. 8.2 if the direction of **B** is defined to be the direction in which the fingers of the right hand curl when the thumb points along the wire in the direction of the (positive) current.

Close to the wire **B** is always at right angles to the wire, in contrast to the electric field, which close to a charge always points toward or away from it. In the electric case, the flux of **E** through a closed surface is proportional to the charge within the volume enclosed by the surface (Gauss's law, Sect. 8.3). In contrast, the flux of **B** through a closed surface is always zero. In the notation of Sect. 4.1,

$$\iint_{\text{closed surface}} B_n\, dS = \iint_{\text{closed surface}} \mathbf{B}\cdot d\mathbf{S} = 0. \tag{8.8}$$

If single magnetic charges (magnetic monopoles) existed, the flux would be proportional to the magnetic charge within the volume. Magnetic monopoles have never been observed, in spite of considerable effort to find them.

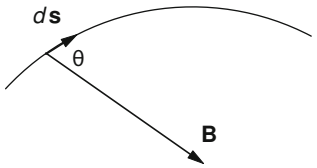

Fig. 8.4 The line integral of $\mathbf{B} \cdot d\mathbf{s}$ is calculated by multiplying $d\mathbf{s}$ by the component of $\mathbf{B}$ parallel to $d\mathbf{s}$, that is $B \cos\theta$

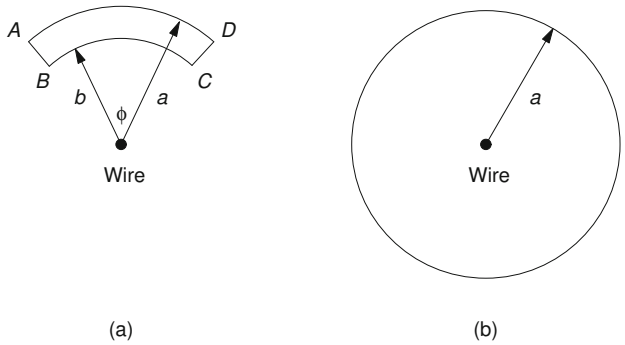

Fig. 8.5 Two paths of integration. In **a** the path does not encircle the wire carrying the current, and $\oint \mathbf{B} \cdot d\mathbf{s} = 0$. In **b** the path encircles the wire and $\oint \mathbf{B} \cdot d\mathbf{s} = \mu_0 i$

As in the electric case, we can construct lines of $\mathbf{B}$. The tangent to the line always points in the direction of $\mathbf{B}$. For the long wire, the lines of $\mathbf{B}$ are circles. One can show from Eq. 8.8 that lines of $\mathbf{B}$ always close on themselves.

Equation 8.8 has the form of the continuity equation, Eq. 4.4, with $\mathbf{B}$ substituted for $\mathbf{j}$ and with $C = 0$. The differential version of Eq. 8.8 can therefore be obtained from Eq. 4.8. It is

$$\text{div}\,\mathbf{B} = \nabla \cdot \mathbf{B} = 0. \tag{8.9}$$

8.2.2 Ampere's Circuital Law

It is also interesting to consider the line integral of $\mathbf{B}$ around a closed path. That is, for any element of the path $d\mathbf{s}$ shown in Fig. 8.4 take the projection of $\mathbf{B}$ in the direction of $d\mathbf{s}$, $B\cos\theta$. Sum up all the contributions $B\cos\theta\, ds$ along the entire closed path. For path $ABCD$ in Fig. 8.5a, the result is zero. The reason is that $B\cos\theta\, ds$ is zero on segments AB and CD. On segment DA it is $(\mu_0 i/2\pi a)(a\phi) = \mu_0 i\phi/2\pi$, while on segment BC it is $-(\mu_0 i/2\pi b)(b\phi) = -\mu_0 i\phi/2\pi$. In Fig. 8.5b the path is circular with the wire at the center, and the line integral is $B(2\pi a) = \mu_0 i$. This result is general:

$$\oint B\cos\theta\, ds = \oint \mathbf{B} \cdot d\mathbf{s} = \mu_0 i. \tag{8.10}$$

The circle on the integral sign means that the integral is taken around a closed path. The line integral of the magnetic field around a closed path is equal to μ_0 times the current through a circuit enclosed by that path. If two wires carrying equal and opposite currents are enclosed by the path of the line integral, the integral is zero. It does *not* mean that $\mathbf{B}$ is zero everywhere on the path.

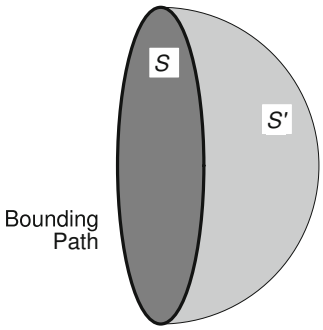

Fig. 8.6 Since the total current or flux of $\mathbf{j}$ through any closed surface is zero, the current through surface S is equal to the current through surface S'

A more general statement is that for steady currents the line integral of $\mathbf{B}$ around a closed path is equal to the integral of the current density $\mathbf{j}$ through any surface enclosed by the path:

$$\oint \mathbf{B} \cdot d\mathbf{s} = \mu_0 \iint \mathbf{j} \cdot d\mathbf{S}. \tag{8.11}$$

This is known as *Ampere's circuital law*. Like Gauss's law, it is always true but not always useful. It is true for currents that do not vary with time, but it can be used to calculate the magnetic field only if symmetry can be used to argue that $\mathbf{B}$ is always parallel to the path and has the same magnitude at all points on the path.

The surface used to calculate the right-hand side can be any surface bounded by the path used on the left. Since we are dealing with steady currents for which there is no charge accumulation, the continuity equation, Eq. 4.4, shows that the flux of $\mathbf{j}$ (the total current) through any closed surface is zero. Two surfaces S and S', both bounded by the path, form a closed surface as shown in Fig. 8.6. The total current through surface S is the same as the total current through S'.

8.2.3 The Biot–Savart Law

In situations where the symmetry of the problem does not allow the field to be calculated from Ampere's law, it is possible to find the field due to a steady current in a closed circuit using the *Biot–Savart law*. The contribution $d\mathbf{B}$ to the magnetic field from current i flowing along a line element $d\mathbf{s}$ is

$$d\mathbf{B} = \frac{\mu_0 i}{4\pi} \frac{d\mathbf{s} \times \mathbf{r}}{r^3}. \tag{8.12}$$

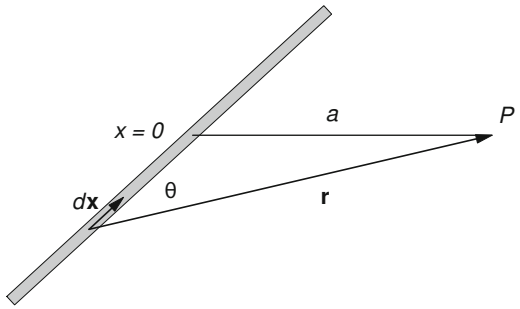

Fig. 8.7 The Biot–Savart law is used to calculate the magnetic field at point P due to an infinite wire

Vector $\mathbf{r}$ is from the current element to the point where the field is to be calculated. The field is found by integrating over the *entire circuit*.

Figure 8.7 shows how this integration is done for an infinitely long straight wire along the x axis. The contribution at point P is obtained by dropping a perpendicular from P to the wire to define $x = 0$. The distance from P to the wire is a. The contribution from an element dx at point x is

$$dB = \frac{\mu_0 i}{4\pi}\frac{dx\ \sin\theta}{r^2} = \frac{\mu_0 i}{4\pi}\frac{a\,dx}{r^3}.$$

Since $r^2 = a^2 + x^2$ the total field is

$$B = \frac{\mu_0 i}{4\pi}\int_{-\infty}^{\infty}\frac{a\,dx}{(a^2+x^2)^{3/2}} = \frac{\mu_0 i a}{4\pi}\left[\frac{x}{a^2(x^2+a^2)^{1/2}}\right]_{-\infty}^{\infty} = \frac{\mu_0 i}{2\pi a}.$$

This agrees with Eq. 8.7 and the result obtained using Ampere's circuital law.

A steady current from a point source which spreads uniformly in all directions generates no magnetic field. To see why consider Fig. 8.8. The source of current is at O. The magnetic field at P can be calculated using the Biot–Savart law. For any element $d\mathbf{s}$ a symmetric element $d\mathbf{s}'$ can be selected, such that $d\mathbf{s} \times \mathbf{r} = -d\mathbf{s}' \times \mathbf{r}'$. Associated with each element is a small area dA, and the current along $d\mathbf{s}$ is $i = j\,dA$. We can set $dA = dA'$ so i is the same in each case. Therefore, $B = 0$. (This can also be shown using Ampere's law; see Problem 11.)

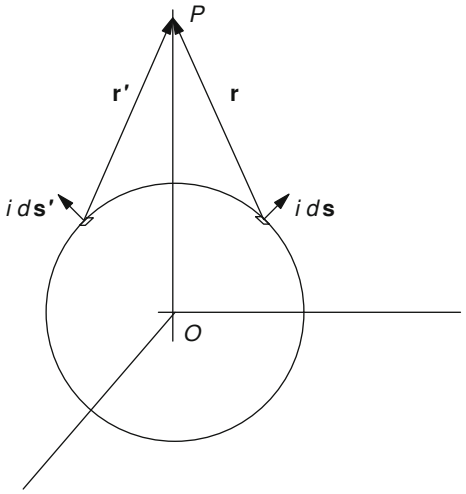

Fig. 8.8 The magnetic field from a spherically symmetric radial distribution of current is zero. The source at O sends current uniformly in all directions. P is the observation point. For any element $d\mathbf{s}$ there is a corresponding $d\mathbf{s}'$ such that $d\mathbf{s}\times\mathbf{r} = -d\mathbf{s}'\times\mathbf{r}'$. The current through a small area dA around $d\mathbf{s}$ is i. The same current flows through a corresponding area around $d\mathbf{s}'$. Can you obtain the same result by a symmetry argument?

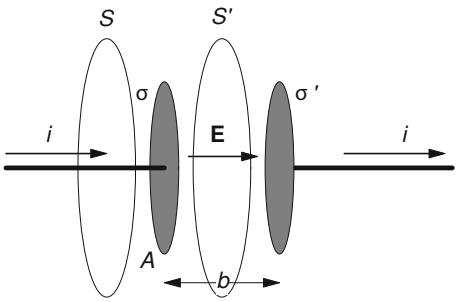

Fig. 8.9 A wire and capacitor plates. The integral of the current density through surface S, which is pierced by the wire, is i. Through surface S', which is between the capacitor plates, the integral is zero. If the displacement current density is included, both surface integrals are the same. (If surfaces S and S' are not large enough, there is also a net displacement current through S, as can be seen from Fig. 8.10)

8.2.4 The Displacement Current

Derivation of Ampere's law requires that there be no charge buildup, so that the total current through a closed surface is zero. However, we will consider an action potential in which the membrane capacitance charges and discharges. To see how this affects Ampere's law, consider current i charging or discharging the two shaded capacitor plates in Fig. 8.9. The area of each capacitor plate is A. The region between the plates, of thickness b, is filled with dielectric of dielectric constant κ. The integral $\iint \mathbf{j}\cdot d\mathbf{S}$ is i for surface S and zero for surface S'. Because of the current, the charge density σ on the left-hand plate is increasing at a rate given by $i = Ad\sigma/dt$, while on the right-hand plate the charge is decreasing because $i = -Ad\sigma/dt$. Since the electric field between the plates is $E = \sigma/\kappa\epsilon_0$ we can say that $i = Ad(\kappa\epsilon_0 E)/dt$. The quantity $D = \kappa\epsilon_0 E$ is called the *electric displacement*, and

$$j_d = \frac{\partial D}{\partial t}$$

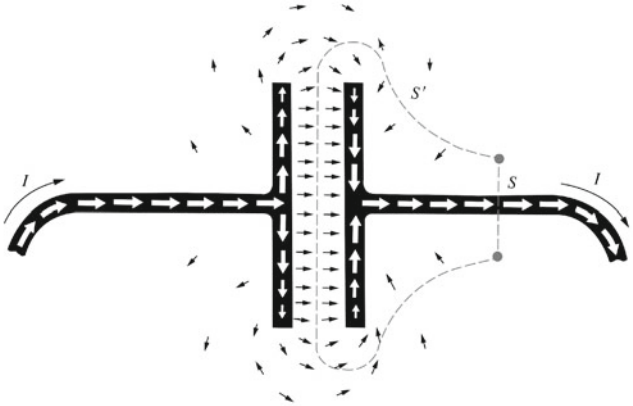

Fig. 8.10 The conduction current (white arrows) and displacement current (black arrows) in a discharging capacitor. The conduction current decreases with distance out the capacitor plates. The displacement current includes the fringing field. (From Purcell and Morin 2013. Used by permission)

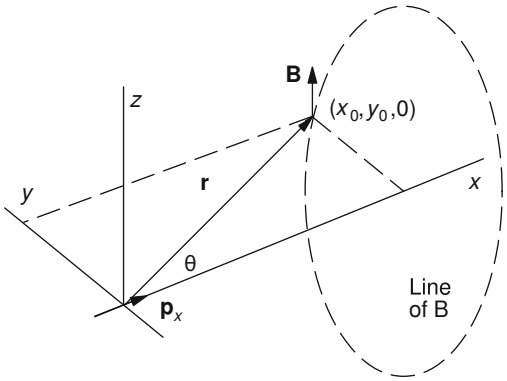

Fig. 8.11 The geometry for calculation of the magnetic field due to a current element $i\,dx$ or current dipole p_x stretched along the x axis

is called the *displacement current density*. More careful consideration shows that Ampere's law is valid when the charge on the plates is changing, if we replace $\mathbf{j}$ by $\mathbf{j} + \mathbf{j}_d$:

$$\oint \mathbf{B} \cdot d\mathbf{s} = \mu_0 \iint (\mathbf{j} + \mathbf{j}_d) \cdot d\mathbf{S}. \tag{8.13}$$

With this change, if S and S' are circles of radius a, Ampere's law gives $B = \mu_0 i/2\pi a$ for either one. (The radius of the circle must be very large; see the discussion in the next paragraph.)

What current should be used in the Biot–Savart law? A very surprising answer is that as long as the fields are relatively slowly varying (so that the emission of radio waves is not important), the displacement current contributes nothing. We are free to include it or ignore it. Purcell and Morin (2013, p. 435) and Shadowitz (1975, p. 416) discuss why this is so. It is not always easy to calculate the entire displacement current. For example, Fig. 8.10 shows how the conduction current and displacement current vary when current charges a capacitor. Notice that some of the displacement current flows to and from the back sides of the capacitor plates. This is why we said in the previous paragraph that the radius of the curve defining surfaces S and S' must be very large in order that one surface has no net flux of displacement current and the other has all of it. Whatever their size, however, Eq. 8.13 is valid.

It was mentioned above that a steady current from a point source that spreads uniformly in all directions generates no magnetic field according to the Biot–Savart law. Yet any circular loop has current flowing through it, so Ampere's law suggests that there is a field. The discrepancy is resolved by noting that the current comes from a charge q at the origin that is being drained off at a rate $i = -dq/dt$. This gives rise to a displacement current $\mathbf{j}_d$ that cancels $\mathbf{j}$ (see Problem 11).

8.3 The Magnetic Field Around an Axon

We can use the Biot–Savart law to calculate the magnetic field due to an action potential propagating down an infinitely long axon stretched along the x axis and embedded in an infinite homogeneous conducting medium. Section 7.1 showed that there are three components to the current: i_i along the interior of the axon, di_o out through the membrane (including both displacement current and conduction current), and current in the surrounding medium.

The principle of superposition allows us to calculate the field due to the exterior current by finding the magnetic field $d\mathbf{B}$ from current di_o into the surrounding medium from axon element dx, and then integrating along the axon. We saw in Chap. 7 that the current in the *external* medium from a small element dx flows uniformly in all directions, as if from a point source. We learned in the preceding section that the magnetic field generated by a spherically symmetric radial current is zero. Therefore, in the approximation that the axon is very thin, we can ignore the external current from each element dx. We can do this only because the medium is infinite, homogeneous, and isotropic. When the exterior conductor has boundaries or structure, the symmetry is broken and the external currents contribute to the magnetic field. Our calculation breaks down very close to the axon. Distortions from the field due to the external current because the axon is not infinitely thin are about 1 % near the axon. The current through the cell membrane gives a very small contribution to the magnetic field—roughly 1 part in 10^6.

The major contribution is therefore from i_i. We use the law of Biot–Savart, Eq. 8.12. The observation point is in the xy plane at $(x_0, y_0, 0)$ and the axon lies along the x axis so that $d\mathbf{s} = \hat{\mathbf{x}}\,dx$, as shown in Fig. 8.11. The product $d\mathbf{s} \times \mathbf{r}$

can be evaluated using Eq. 1.8 or 1.9:

$$d\mathbf{s} \times \mathbf{r} = \begin{vmatrix} \hat{\mathbf{x}} & \hat{\mathbf{y}} & \hat{\mathbf{z}} \\ dx & 0 & 0 \\ x_0 - x & y_0 & 0 \end{vmatrix} = dx\, y_0\, \hat{\mathbf{z}}.$$

The term in the denominator is $r^3 = \left[(x_0 - x)^2 + y_0^2\right]^{3/2}$. The magnetic field in the xy plane is in the z direction and has magnitude

$$B_z = \frac{\mu_0 y_0}{4\pi} \int \frac{i_i(x)\, dx}{\left[(x_0 - x)^2 + y_0^2\right]^{3/2}}.$$

It was shown in Eqs. 7.17 that $i_i = -\pi a^2 \sigma_i (dv_i/dx)$. The final expression for B_z is

$$B_z = -\frac{\mu_0 a^2 \sigma_i y_0}{4} \int \frac{\left[dv_i(x)/dx\right] dx}{\left[(x_0 - x)^2 + y_0^2\right]^{3/2}}. \tag{8.14}$$

The computer program in Fig. 8.12 evaluates the field for the same crayfish axon whose external potential was studied in Sect. 7.4. The field at a distance $2a$ from the axon is plotted in Fig. 8.13. The results agree well with more sophisticated calculations (Swinney and Wikswo 1980; Woosley et al. 1985). The latter reference is particularly clear and should be accessible to those who have studied the convolution integral in Chap. 12. A three-dimensional plot of their results is shown in Fig. 8.14.

It is worth repeating that a calculation this simple succeeds only because the axon and the exterior medium are infinite. If there are boundaries, or if there are regions in the external medium where the conductivity changes, then current in the external medium does contribute to the magnetic field. For example, an isolated nerve preparation in air would have the external current flowing in a thin layer of ionic solution along the outside of the axon, where it would generate a field that almost completely cancels that from i_i.

An approximation valid at large distances can be obtained from Eq. 8.14 by expanding the denominator in much the same way we did to obtain Eqs. 7.26 and 7.27. The observation point is (R, θ) in the xy plane. In this case we need the expansion of

$$\frac{1}{r^3} = \frac{1}{R^3}\left(1 - 2\frac{x}{R}\cos\theta + \frac{x^2}{R^2}\right)^{-3/2} \approx \frac{1}{R^3}\left(1 + \frac{3x\cos\theta}{R} + \cdots\right).$$

The final result is

$$B_z = \frac{\mu_0\, \pi a^2\, \sigma_i \sin\theta}{4\pi R^2}\left(v_i(x_1) - v_i(x_2)\right) + \frac{\mu_0\, \pi a^2\, \sigma_i 3 \sin\theta\cos\theta}{4\pi R^3}\left[-x v_i(x)\big|_{x_1}^{x_2} + \int_{x_1}^{x_2} v_i(x)\, dx\right]. \tag{8.15}$$

The first term is proportional to the current dipole, $\mathbf{p}$, defined for the depolarization in the previous chapter. For a complete pulse the first term vanishes and the second term is used.

8.4 The Magnetocardiogram

It is now feasible to measure magnetic fields arising from the electrical activity of the heart (the *magnetocardiogram* or *MCG*) and the brain (the *magnetoencephalogram* or *MEG*). The models developed in Sect. 8.3 and in Chap. 7 can be used to compare the electric and magnetic signals from a current dipole $\mathbf{p}$. The instrumentation for these measurements is described in Sect. 8.9.

For a single cell at the origin in a homogeneous conducting medium, the exterior potential at observation point $\mathbf{r}$ is given by Eq. 7.13:

$$v = \frac{\mathbf{p} \cdot \mathbf{r}}{4\pi\sigma_o r^3}.$$

The current dipole $\mathbf{p}$ points along the cell in the direction of the advancing depolarization wave and has magnitude (Eq. 7.12) $p = \pi a^2 \sigma_i \Delta v_i$. An expression analogous to Eq. 7.13 describes the magnetic field of a depolarizing cell. We consider the field due to current along the x axis and then generalize the result. The derivation begins with Eq. 8.15 and uses the geometry of Fig. 8.11. The region of depolarization occupies only a millimeter or so along the cell. Since the measurements are made much farther away, the denominator can be removed from the integral, which is then just $\int (dv/dx)\, dx$. If the depolarization is at the origin, then the expression for B_z for $z = 0$ is

$$B_z = -\frac{\mu_0 a^2 \sigma_i y_0 \left[v(x_2) - v(x_1)\right]}{4(x_0^2 + y_0^2)^{3/2}} = \frac{\mu_0}{4\pi}\frac{p y_0}{(x_0^2 + y_0^2)^{3/2}}. \tag{8.16}$$

Figure 8.11 shows that $y_0 = r\sin\theta$, so that $p y_0 = p\, r \sin\theta = |\mathbf{p} \times \mathbf{r}|$. The direction of $\mathbf{B}$ is also consistent with the cross product. Generalizing, we have for a single cell,

$$\mathbf{B} = \mu_0 \frac{\mathbf{p} \times \mathbf{r}}{4\pi r^3}. \tag{8.17}$$

Note the remarkable similarity between Eqs. 7.13 and 8.17. One involves the dot product, and the other the cross product. For both, the field falls as $1/r^2$. If we are considering the cardiogram, either field from the entire heart is the superposition of the field from many cells. As with the electrocardiogram, the first approximation for the magnetocardiogram is to ignore changes in $1/r^2$ and speak of the total current-dipole vector.

Measurements of either the potential or the magnetic field can be used to determine the location of $\mathbf{p}$. We will adopt the coordinate system usually used for the magnetocardiogram.

```
/*This program integrates to
obtain the magnetic field for
a problem which was first
solved by K. R. Swinney and J.
P. Wikswo, the extracellular
magnetic field of the single
active nerve fiber in a volume
conductor. Biophys. J. 32:719-732
(1980). The nerve pulse is
a series of Gaussians used by
Clark and Plonsey to fit the
data of Watanabe and Grund-
fest, J. Gen. Physiol. 45:267
(1961). Uses Romberg integra-
tion routine qromb from W. H.
Press et al. Numerical Recipes
in C.*/

#include <stdio.h>
#include <stdlib.h>
#include <math.h>
#include "nr.h"

/*Global Variables*/
const double pi = 3.14159265359;
double x0, y0,  //coordinates
 of observation point
A[3], B[3], C[3];//parameters
for gaussian
float f(float x)
{
/*Calculates the integrand
dv/dx divided by r^3*/
  double xx, r, dv;
  int i;
  dv = 0;
  for (i=0; i<3; i++)
  {  xx = B[i] * (x- C[i]);
    dv = dv-2 * A[i] * B[i] *
          xx * exp(-xx * xx);}
  r = sqrt((x0 - x) * (x0 - x)
     + y0 * y0);
  return dv / (r * r * r);
}
void main()
{
  FILE *ofp;//output file pointer
  const double Mu0 = 4.0e-7 *
pi,  //permeability free space
  axonradius = 6.0e-5,
  xstart = 0.0,
  xfinish = 0.020;
double integral, MagField,
    y[4];

//Calculate at four different
distances
//from axon
int i;

  if (!(ofp =
fopen("OutputFile","w")))
  {printf("cannnot open output
file\n");  exit(1);}
  A[0] = 0.051;
  A[1] = 0.072;
  A[2] = 0.018;
  B[0] = 800;
  B[1] = 533;
  B[2] = 333;
  C[0] = 0.0054;
  C[1] = 0.0066;
  C[2] = 0.0086;
  y[0] = 2 * axonradius;
  y[1] = 0.001;
  y[2] = 0.003;
  y[3] = 0.01;
printf("%12.5g %12.5g %12.5g
%12.5g\n",
y[0],y[1],y[2],y[3]);
fprintf(ofp, "%12.5g\t
%12.5g\t%12.5g\t%12.5g\n",
y[0],y[1],y[2],y[3]);
  for(x0 = xstart; x0<xfinish;
x0+=0.00025)
  {
    printf("%12.5f",x0);
    fprintf(ofp,"%12.5f",x0);
    for(i=0; i<4; i++)
    {
      y0 = y[i];
      integral = qromb(f,
xstart, xfinish);
      MagField = -Mu0 *
axonradius * axonradius * y0 *
integral / 4.0;
      printf("%12.5e",MagField);
  fprintf(ofp,"\t%12g",MagField);
    }
    printf("\n");
    fprintf(ofp,"\n");
  }
  fclose(ofp);
}
```

Fig. 8.12 The program used to calculate the magnetic field outside an axon in an infinite homogeneous conductor using Eq. 8.14. It uses the Romberg integration routine `qromb` from Press et al. (1992)

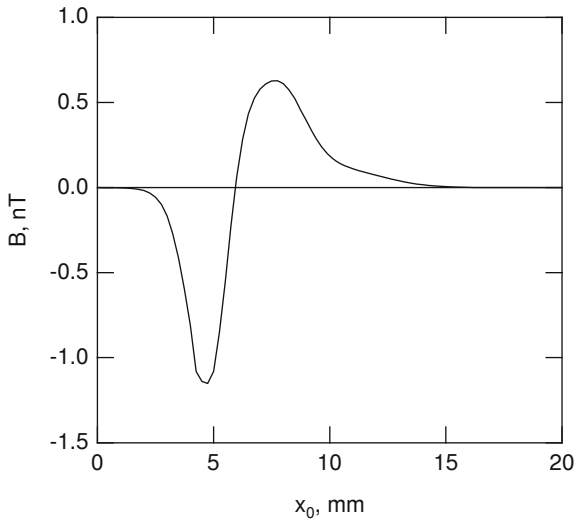

Fig. 8.13 The magnetic field B_z 0.12 mm from a crayfish axon in an infinite homogeneous conducting medium is shown. The field was calculated using the program of Fig. 8.12. The exterior potential for this configuration was calculated in Sect. 7.4

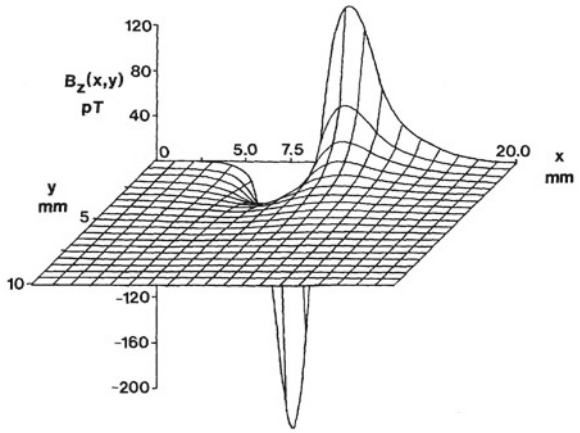

Fig. 8.14 A three-dimensional plot of the magnetic field around the crayfish axon. The minimum distance from the axon is 0.5 mm

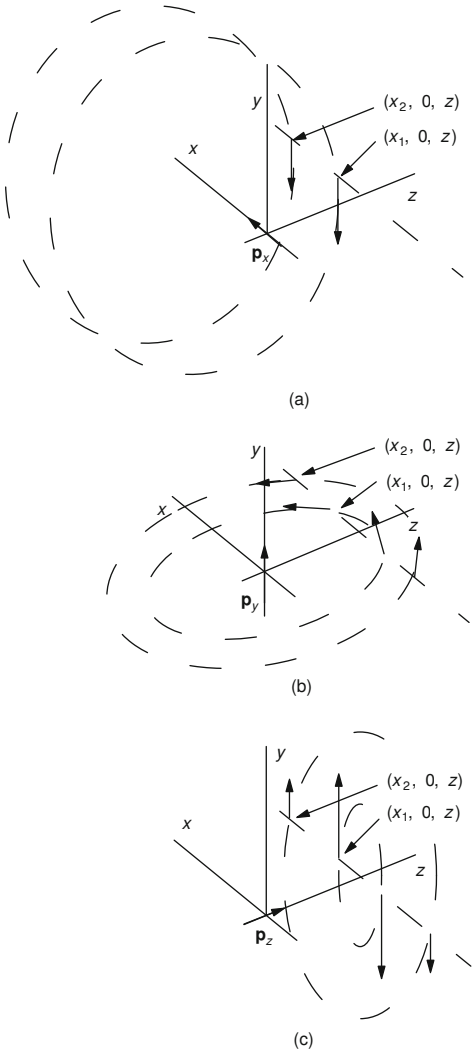

Fig. 8.15 The magnetic field produced by the three components of a current dipole at the origin. The coordinate system is that customarily used for magnetocardiography. The x axis points toward the subject's left, the y axis is vertical, and the z axis points forward through the subject's chest. The coordinate system is viewed over the subject's right shoulder

The x axis points to the patient's left, the y axis points up, and the z axis points toward the front of the patient, roughly perpendicular to the chest wall. Assume that **p** is at the origin and the anterior chest surface is the xy plane at some fixed value of z. We ignore distortions to the field which arise because no current can flow in the region beyond the body, and we assume that the conductivity of the body is homogeneous and isotropic. From Eq. 8.17, we obtain the three components of **B** along the line $(x, 0, z)$:

$$B_x = \frac{\mu_0 p_y z}{4\pi r^3},$$
$$B_y = \frac{\mu_0 (p_z x - z p_x)}{4\pi r^3}, \tag{8.18}$$
$$B_z = -\frac{\mu_0 p_y x}{4\pi r^3}.$$

Compare these results to the lines of **B** in Fig. 8.15, which were drawn for the three components of **p** using the right-hand rule. Along the line being considered ($y = 0, z =$ const), p_x contributes only to B_y, and B_y is always negative. Component p_y contributes to both B_x and B_z; the latter

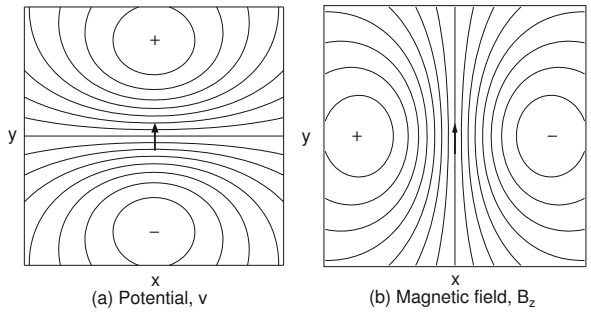

Fig. 8.16 Contour plots in the xy plane for **a** the potential and **b** the z component of the magnetic field from a current dipole **p** pointing along the y axis, calculated for an infinite, isotropic conducting medium

changes sign while the former does not, as we change the value of x. Component p_z gives only a y component of **B** that changes sign as x changes sign. The component normal to the body surface, B_z is given by

$$B_z(x, 0, z) = -\frac{\mu_0}{4\pi} \frac{p_y x}{(x^2 + z^2)^{3/2}}.$$

Figure 8.16 plots contours for the potential and the magnetic field component B_z perpendicular to the body surface when **p** points along the y axis. Again, distortions because of changes in conductivity are ignored. The similarity of the two sets of contours is clear. The contours of constant potential are proportional to $p_y y/r^3$, while the contours for B_z are proportional to $-p_y x/r^3$. Either contour map can be used to determine the location and depth of **p**. To be specific, consider the contours for B_z. The field is proportional to the function $x/(x^2 + z^2)^{3/2}$, which changes sign right over the source and has a maximum and a minimum at $x = \pm z/\sqrt{2}$. The depth of the source z is related to the spacing Δx along the x axis between the maximum and minimum by

$$z = \frac{\Delta x}{\sqrt{2}}. \tag{8.19}$$

The source is located directly beneath the point on the axis where $B_z = 0$, and its strength is related to the maximum value of B_z by

$$B_z(\max) = \frac{\mu_0 p_y}{6\pi\sqrt{3}z^2}. \tag{8.20}$$

Figure 8.17 shows real maps of the potential and the magnetic field on the surface of the chest. While the basic features are described by the simple current dipole model, the exact shape of the contours in Fig. 8.17 differs from the shape in Fig. 8.16. This is due to variations in conductivity of the body. The surface potential is distorted by conductivity differences throughout the thorax; the magnetic field is particularly susceptible to return currents flowing just below the surface of the body. Hosaka et al. (1976) did an early calculation of the effect of currents at the surface of the torso

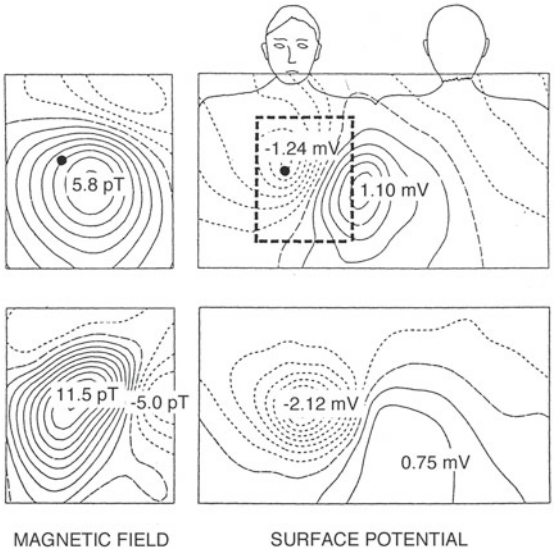

Fig. 8.17 The 56-lead magnetic field map of B_z (left) and the 117-lead potential map (right) during the R-wave maximum for a normal subject (top row) and a patient with an anterior myocardial infarction (bottom row). The maximum and minimum values of each map are indicated on each map. B_z oriented into the page is defined as positive (solid lines) The dashed rectangle in the potential map corresponds to the area for which the magnetic field was measured. The dot in the upper row shows where the midline intersects the level of the fourth intercostal space. Note how the constant contours for the magnetic field are oriented at right angles to the isopotential lines, as in the previous figure. Modified from Stroink (1992) Used by permission

on the magnetocardiogram. They found that the return current modifies the component of **B** perpendicular to the body surface by about 30 %. Tangential components of **B** are influenced more; this is why the normal component B_z is usually measured. Tan et al. (1992) show that using a model of the conductivities that matches the geometry of the patient's thorax allows accurate localization of the current dipole source from the surface measurements. The magnetocardiogram is now being used to record fetal heart arrhythmias (Strasburger et al. 2008).

The magnetic field close to the heart is affected by the anisotropy of the tissue conductivity. Figure 8.18 shows measurements made 1.5 mm from a 1-mm-thick slice of canine myocardium by Staton et al. (1993). Panel A shows the time course of simultaneous recordings from three pickup coils 3 mm in diameter and separated by 4 mm. There are striking differences over 4 mm. Panel B shows a magnetic field contour map during stimulus from another experiment. Instead of having one peak and one valley as in Figs. 8.16 and 8.17, it shows a cloverleaf or *quatrefoil* pattern. Panels C and D show the field contours and the current flow in a third experiment, 6 ms after stimulation. This field and current pattern is predicted by bidomain calculations (Wikswo 1995b).

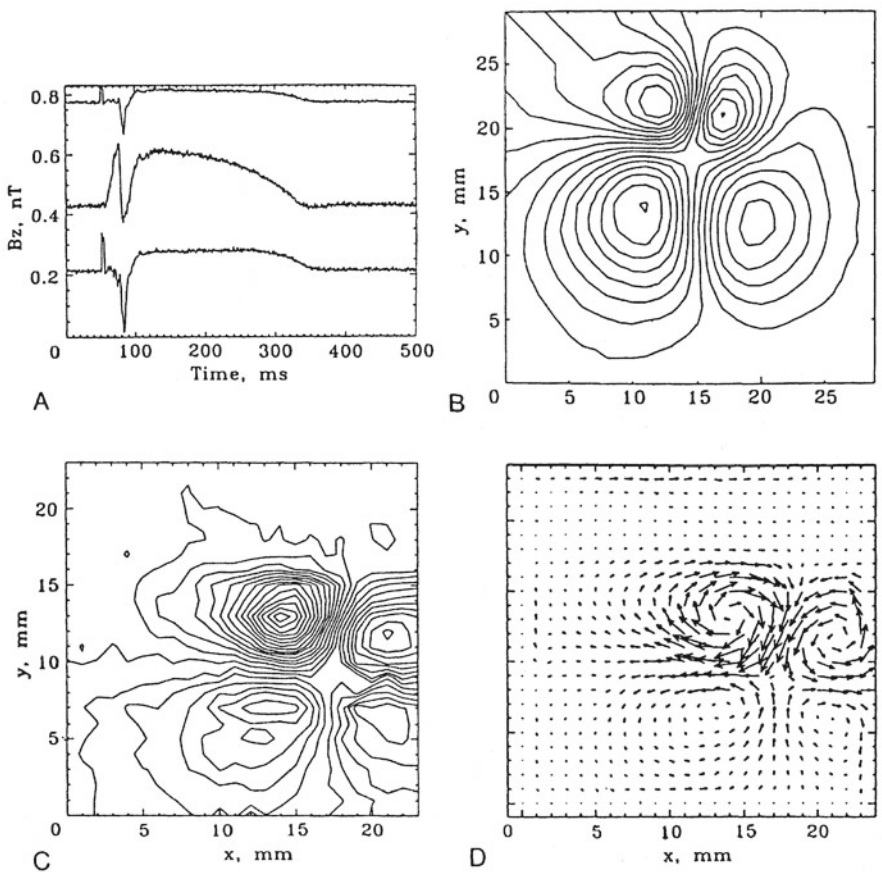

Fig. 8.18 The results of magnetic field measurements very close to a slice of canine myocardium. The panels are described in the text. Part of the figure is reproduced from Wikswo 1995b ©1995 Elsevier, Inc, with permission of Elsevier. The rest is from Staton et al. (1993), ©1993 IEEE

8.5 The Magnetoencephalogram

The magnetic signals from a nerve action potential are weaker than those from the heart for two reasons. First, the current-dipole vector associated with the repolarization follows close behind the depolarization and reduces the field. (The largest unmyelinated axons in the body have a conduction speed of about 1 m s^{-1} and the pulse is about 1 mm long. Myelinated fibers have a pulse length up to 80–100 times longer.) Second, the cross-sectional area of the advancing wavefront is much smaller. However, the magnetic fields accompanying action potentials have been measured in nerve (Barach et al. 1985; Roth and Wikswo 1985) and in muscle (Gielen et al. 1991). They have also been measured in green algae (Trontelj et al. 1994).

We saw in Sect. 6.1 that nerve cells have an input end (dendrites), a cell body, and an axon. The signal that propagates from a synapse through the dendrites to the cell body and axon is much smaller (about 10 mV) and longer (10 ms) than an action potential that travels along the axon. The cells at the surface of the cerebral cortex have dendrites that are like the trunk of a tree perpendicular to the surface of the cortex, with branches from several directions coming to the trunk. The signal from the trunk is the primary contributor to the magnetoencephalogram (MEG) and electroencephalogram (EEG). The problems show that the magnetic field associated with the rise of the postsynaptic potential is more easily observed outside the brain than is the action potential.

One can see from the symmetry argument in the caption of Fig. 8.19 that in a spherically symmetric conducting medium the radial component of **p** and its return currents do not generate any magnetic field outside the sphere. Therefore the MEG is most sensitive to detecting activity in the fissures of the cortex, where the trunk of the postsynaptic dendrite is perpendicular to the surface of the fissure. A tangential component of **p** does produce a magnetic field outside a spherically symmetric conductor. The extracellular current does not contribute to the radial component of the magnetic field (Hämäläinen et al. 1993), so Eq. 8.17 gives B_r

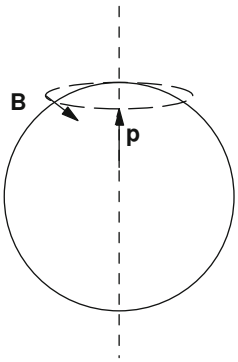

Fig. 8.19 A current dipole **p** is oriented radially inside a homogeneous conducting sphere. The return current is independent of the azimuthal angle, ϕ. By symmetry the magnetic field, if any, must be in the ϕ direction; the current in Ampere's circuital law, which is the sum of the current in p and the return current, is zero

correctly. Extracellular current does influence the tangential components of the magnetic field. Since the skull is not a perfect sphere, there is some effect of the radial component of **p** on the MEG. The EEG is sensitive to both radial and tangential components of **p**. The information available from the EEG and MEG has been reviewed by Wikswo et al. (1993).

In the last decade, the use of the MEG has grown dramatically for conditions such as epilepsy, stroke, chronic pain, and dyslexia (Hari and Salmelin 2012).

Measurements of the magnetoencephalogram are often based on evoked responses. A repetitive stimulus—audible, visual, or tactile—is presented to the subject or the subject is asked to perform a repetitive task such as flexing a finger. Signal-averaging techniques are used to identify the associated changes in magnetic field (see Chap. 11). Figure 8.20 shows averaged magnetic field contours measured over the scalp of a subject who heard a string of words presented in random order every 2.3 s. Sometimes the subject was asked to read something else and ignore the words. At other times the subject was asked to pay attention and count how many of the words were on a list. The first peak, 100 ms after presentation of the word, was the same in both cases. The sustained field peak, SF, was considerably stronger when the subject was paying attention to the list. Magnetic contours and the equivalent current dipole source are also shown.

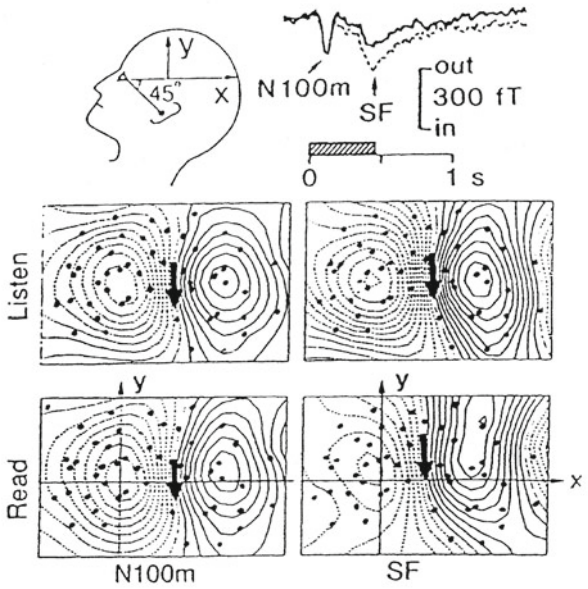

Fig. 8.20 Magnetic field maps recorded over the scalp of a subject who heard a series of words and either ignored them by reading something else or listened carefully and counted how many of the words were in a predetermined list. The features are discussed in the text. Reprinted with permission from Hämäläinen et al. 1993. Copyright © 1993 by the American Physical Society

8.6 Electromagnetic Induction

In 1831 Michael Faraday discovered that a *changing* magnetic field causes an electric current to flow in a circuit. It does not matter whether the magnetic field is from a permanent magnet moving with respect to the circuit or from the changing current in another circuit. The results of many experiments can be summarized in the *Faraday induction law*:

$$\oint \mathbf{E}\cdot d\mathbf{s} = -\frac{d}{dt}\iint \mathbf{B}\cdot d\mathbf{S} = -\frac{d\Phi}{dt}. \tag{8.21}$$

It states that the line integral of **E** around a closed path is equal to minus the rate of change of the magnetic flux through any surface bounded by the path. The relationship between the direction of **S** and $d\mathbf{s}$ is given by a right-hand rule: if the fingers of the right hand curl around the circuit in the direction of $d\mathbf{s}$, the thumb of the right hand points in the direction of a positive normal to **S**. The units of magnetic flux $\Phi = \iint \mathbf{B}\cdot d\mathbf{S}$ are T m^2 or weber (Wb). Rapidly changing magnetic fields can induce currents large enough to trigger nerve impulses. This is discussed in Sect. 8.7.

The differential form of the Faraday induction law is (see Problem 22)

$$\operatorname{curl}\mathbf{E} = \nabla\times\mathbf{E} = -\frac{\partial\mathbf{B}}{\partial t}. \tag{8.22}$$

The result of the vector operation *curl* is another vector. In Cartesian coordinates the components of $\nabla\times\mathbf{E}$ are

$$(\nabla\times\mathbf{E})_x = \frac{\partial E_z}{\partial y} - \frac{\partial E_y}{\partial z},$$
$$(\nabla\times\mathbf{E})_y = \frac{\partial E_x}{\partial z} - \frac{\partial E_z}{\partial x},$$
$$(\nabla\times\mathbf{E})_z = \frac{\partial E_y}{\partial x} - \frac{\partial E_x}{\partial y}.$$

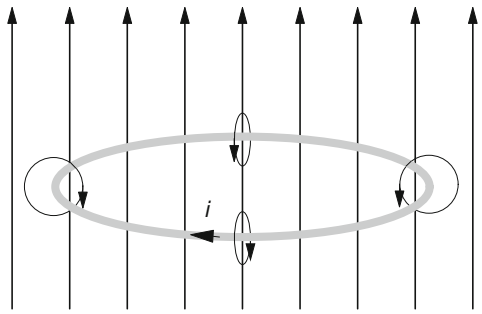

Fig. 8.21 A magnetic field increasing in the direction shown induces a current in the loop. This current generates a magnetic field in the opposite direction, opposing the change in the magnetic field

These can be abbreviated by using determinant notation as

$$(\nabla \times \mathbf{E}) = \begin{vmatrix} \hat{\mathbf{x}} & \hat{\mathbf{y}} & \hat{\mathbf{z}} \\ \dfrac{\partial}{\partial x} & \dfrac{\partial}{\partial y} & \dfrac{\partial}{\partial z} \\ E_x & E_y & E_z \end{vmatrix}. \tag{8.23}$$

Similarly (Problem 23) the differential form of Ampere's law is

$$\operatorname{curl} \mathbf{B} = \nabla \times \mathbf{B} = \mu_0 \left(\mathbf{j} + \frac{\partial \mathbf{D}}{\partial t} \right). \tag{8.24}$$

The integral form of the Faraday induction law can be used to determine $\mathbf{E}$ only if the symmetry is such that $\mathbf{E}$ is always parallel to $d\mathbf{s}$ and has the same magnitude all along the path. One situation where it can be used is a circular loop of wire in the xy plane centered at the origin. The radius of the loop is a and its normal is along the $+z$ axis. Suppose that everywhere in the xy plane within the boundary of the circle the field points along z and depends only on time: $\mathbf{B}(x, y, z, t) = B(t)\hat{\mathbf{z}}$. Symmetry shows that $\mathbf{E}$ has the same magnitude everywhere in the wire and is always tangent to the loop. Equation 8.21 gives

$$E = -\frac{a}{2}\frac{dB}{dt}. \tag{8.25}$$

If the loop is made of material that obeys Ohm's law, there is a current of density $j = \sigma E = -(\sigma a/2)(dB/dt)$. If the radius of the wire is b ($b \ll a$), then $i = -(\sigma \pi a b^2/2)(dB/dt)$. Figure 8.21 shows the direction of the induced current if dB/dt is positive. The induced current sets up its own magnetic field which points in the $-z$ direction within the loop, opposing the primary field increase within the loop. The induced current always opposes the *change* of magnetic field that produces it. This is called *Lenz's law*. If it were not true, the induced current, once started, would increase indefinitely.

This result does not require that the ring be hollow; it can be part of a much larger conductor. The larger the conductor, the greater the radius of the path along which the induced current can flow. The currents that changing magnetic fields induce in conductors are called *eddy currents* and cause heating losses in the conductor. Iron, which is a conductor, is often used as a core in transformer windings to increase the intensity of the magnetic field. To reduce the eddy-current losses, the cores are made of thin layers of iron insulated from one another by varnish. This limits the radius of the path in which the eddy currents can flow. Some coils and transformers are wound on cores of powdered iron dispersed in an insulating binder. Rooms with thick conducting walls (aluminum, about 2-cm thick) have been used to shield against 60-Hz magnetic fields from power wiring. The eddy currents induced in the aluminum attenuate the field by about a factor of 200 (Stroink et al. (1981)).

The quantity $\int_a^b \mathbf{E} \cdot d\mathbf{s}$ is the work done per unit charge in moving from a to b and is called the *electromotive force along the path from a to b*. Terminology is not always consistent; see the discussion by Page (1977). The details of how a changing magnetic field causes a current to flow were shown above for a circular conductor. The force on a moving charge due to the induced electric field is balanced by the drag force as the charge drifts through the conductor. Energy supplied by the changing magnetic field is dissipated as heat. If a voltmeter is attached to two points on the circle, the voltmeter reading may seem paradoxical, until one realizes that there may be changing flux in the voltmeter leads as well. An additional complication is that when there is any region of space in which $\nabla \times \mathbf{E} \neq 0$, then it is possible for $\int_a^b \mathbf{E} \cdot d\mathbf{s}$ to depend on the path (rather than just the end points), even if the magnetic field is zero at all points on the path. This is described clearly and in detail by Romer (1982).

8.7 Magnetic Stimulation

Since a changing magnetic field generates an induced electric field, it is possible to stimulate nerve or muscle cells without using electrodes. The advantage is that for a given induced current deep within the brain, the currents in the scalp that are induced by the magnetic field are far less than the currents that would be required for electrical stimulation. Therefore *transcranial magnetic stimulation* (TMS) is relatively painless. It is also safe (Rossi et al. 2009).

Magnetic stimulation can be used to diagnose central nervous system diseases that slow the conduction velocity in motor nerves without changing the conduction velocity in sensory nerves (Hallett and Cohen 1989). It could be used to monitor motor nerves during spinal cord surgery, and to map motor brain function. Because TMS is noninvasive and nearly painless, it can be used to study learning and plasticity (changes in brain organization over time; Wassermann

et al. 2008). Recently, researchers have suggested that repetitive TMS might be useful for treating disorders such as depression (O'Reardon et al. 2007) and Alzheimer's disease (Freitas et al. 2011).

One of the earliest investigations was reported by Barker, Jalinous and Freeston (1985). They used a solenoid in which the magnetic field changed by 2 T in 110 μs to apply a stimulus to different points on a subject's arm and skull. The stimulus made a subject's finger twitch after the delay required for the nerve impulse to travel to the muscle. For a region of radius $a = 10\,\text{mm}$ in material of conductivity $1\ \text{S m}^{-1}$, the induced current density for the field change in Barker's solenoid was $90\ \text{A m}^{-2}$. (This is for conducting material inside the solenoid; the field falls off outside the solenoid, so the induced current is less.) This current density is large compared to current densities in nerves (Chap. 6).

Magnetic stimulators are relatively high-power devices, requiring thousands of amps passed through coils for a few hundred microseconds. Most magnetic stimulators are capacitor discharge devices, in which a large capacitor is charged to a high voltage (several kV) and then discharged through the coil. Different coil geometries have been examined; the most common one is a figure-of-eight shape. Magnetic stimulation is included in the review by Roth (1994) and is compared to other brain imaging methods by Ilmoniemi et al. (1999).

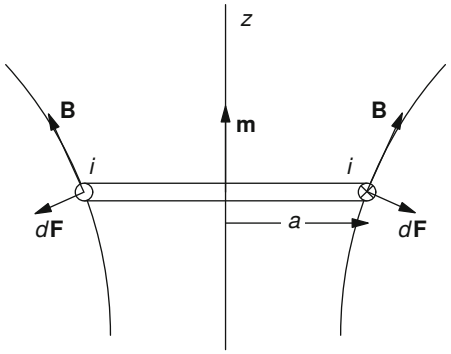

Fig. 8.22 A current loop in an inhomogeneous magnetic field experiences a force toward the region of stronger magnetic field. The circular loop lies in a plane perpendicular to the z axis. Current flows into the page on the *right* and out of the page on the *left*

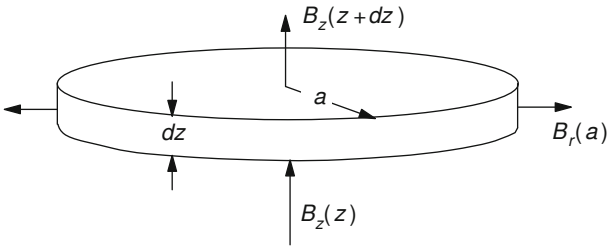

Fig. 8.23 Gauss's law for **B** is applied to a pillbox of radius a and thickness dz

8.8 Magnetic Materials and Biological Systems

Just as the electric field can be altered by the polarization of a dielectric, the magnetic field can be altered by matter. Biological measurements can be based on alterations of the field by an organ in the body. Some cells exhibit permanent magnetism, which is important for measuring direction in some bacteria, birds, and other organisms.

8.8.1 Magnetic Materials

The effects of magnetic fields on material are more complicated than those of electric fields. Since there are no known magnetic charges (monopoles), we must consider the effect of magnetic fields on current loops or magnetic dipoles. Figure 8.22 shows a current loop in a magnetic field that decreases as z increases. As a result the lines of **B** spread apart. The loop has radius a, carries current i, and has magnetic moment[1] **m**. For the orientation shown, there is a force on the loop in the $-z$ direction that is toward the region where the field is stronger. If the magnetic moment of the loop were not parallel to **B**, there would also be a torque on the loop. For ease in calculation, imagine that the loop has been placed in the field in such a way that along the axis of the loop, **B** points in the z direction. Then the spreading of the lines of **B** means that **B** has a component radially outward all around the loop. Because of the symmetry B_r has a constant magnitude everywhere around the loop, and the force on the loop is $-2\pi a\, i\, B_r(a)$.

Field $B_r(a)$ is found by considering the fact that the total magnetic flux through all surfaces of the pillbox in Fig. 8.23 is zero (Eq. 8.8). The net outward flux is

$$\left[B_z(z+dz) - B_z(z)\right]\pi a^2 + B_r(a)2\pi a\, dz = 0.$$

This can be rearranged to give

$$\left[\frac{\partial B_z}{\partial z} + \frac{2}{a}B_r(a)\right]\pi a^2\, dz = 0,$$

from which

$$B_r(a) = -\frac{a}{2}\frac{\partial B_z}{\partial z}.$$

[1] Be careful. We are talking about two different kinds of dipoles in this chapter. The current dipole **p** is a source and sink of current and has units A m. The magnetic dipole **m**, equivalent to a small magnet with north and south poles, has units A m^2. The magnetic field from a magnetic dipole falls off as $1/r^3$.

The force on the loop is therefore

$$F_z = \pi a^2 i \frac{\partial B_z}{\partial z} = m_z \frac{\partial B_z}{\partial z}. \tag{8.26}$$

If **m** is parallel to **B** the force is toward the region of stronger field; if **m** is antiparallel to **B** the force is toward the region of weaker field.

An atom can have a magnetic moment because of two effects.[2] The motion of the electrons in orbit about the nucleus constitutes a current, as a result of which there may be an *orbital magnetic moment*. The intrinsic *spin* of each electron gives rise to a spin magnetic moment, independent of any orbital motion. In most atoms, the orbital magnetic moments average to zero, and most of the electrons are arranged in pairs whose spins cancel. The atom therefore usually has no net magnetic moment.

Most substances placed in an inhomogeneous field experience a weak force *away* from the region of strong field, and the force is roughly proportional to the square of the field strength, an effect called *diamagnetism*. It can be understood with a simple classical model. As the atom is moved into the magnetic field, the Faraday induction effect distorts the orbits of the electrons to induce a magnetic dipole moment proportional to **B** and in the opposite direction, consistent with Lenz's law. The force is therefore proportional to $B_z(\partial B_z/\partial z)$.

A few substances are *attracted* to the region of stronger field, again with a force that is often proportional to the square of the field. Each atom of these *paramagnetic* substances has a permanent magnetic moment associated with the spin of an unpaired electron. Thermal motion normally keeps the magnetic moments of different atoms oriented randomly. As the substance is brought into the magnetic field the spin magnetic moments of different atoms begin to align with the magnetic field. A magnetic dipole moment is induced in the substance, but this time it is in the direction of **B**, and the substance is attracted to the magnet.

Some substances placed in an inhomogeneous magnetic field experience much stronger attraction than do paramagnetic substances. In these substances some of the atomic moments are aligned even in the absence of an external field. They are permanent magnets. Further alignment of the atomic moments may take place in an external field, but complete alignment often takes place in relatively weak external fields. These substances are called *ferromagnets*. The individual atoms have magnetic moments, and there are forces between atoms that cause the spins to align. Section 14-4 of Eisberg and Resnick (1985) provides a relatively simple explanation of the quantum-mechanical effects underlying this spin alignment and the formation of microscopic regions of aligned spins called *domains*. *Ferrimagnets* are similar to ferromagnets, but the crystals contain two different kinds of ions with different magnetic moments.

The *magnetization* **M** is the average magnetic moment per unit volume. It is defined by considering volume ΔV that has total magnetic moment $\Delta\mathbf{m} = \sum \mathbf{m}_i$, where the summation is taken over all atoms in the volume, and taking the ratio

$$\mathbf{M} = \frac{\Delta\mathbf{m}}{\Delta V}. \tag{8.27}$$

We have seen that a current loop possesses a magnetic moment of magnitude $m = iS$. One can imagine a current giving rise to any magnetic moment, even one associated with electron spin. Such currents are called *bound currents* and must be included in Ampere's law. The currents that flow due to conduction—that we can control by changing the conductivity of the material or throwing a switch—are called *free currents*. One can show that if we define the new vector

$$\mathbf{H} = \mathbf{B}/\mu_0 - \mathbf{M}, \tag{8.28}$$

it depends only on the free currents:

$$\oint \mathbf{H} \cdot d\mathbf{s} = \iint \mathbf{j}_{\text{free}} \cdot d\mathbf{S}. \tag{8.29}$$

Vector **H** is called the *magnetic field intensity*. It has units A m^{-1}. It does not have the physical significance of **B** (it does not appear in the Lorentz force or the Faraday induction law). However, it often simplifies computations, because we control free current in the laboratory.

In a vacuum, $\mathbf{B} = \mu_0\mathbf{H}$. It has been traditional to define the *magnetic permeability* of a medium in which **B**, **M**, and **H** are all proportional to one another by the equation

$$\mathbf{B} = \mu\mathbf{H}, \tag{8.30}$$

in which case

$$\frac{\mu}{\mu_0} = 1 + \frac{M}{H} = 1 + \chi_m. \tag{8.31}$$

In diamagnetic materials the *magnetic susceptibility* χ_m is negative and $\mu < \mu_0$. A typical diamagnetic susceptibility is $\approx -1 \times 10^{-5}$. In paramagnetic materials χ_m is positive and $\mu > \mu_0$. A typical paramagnetic susceptibility is $\approx 1 \times 10^{-4}$.

The relationship between B and H in ferromagnetic substances is nonlinear and is characterized by a BH curve. A typical curve is shown in Fig. 8.24. The fact that the curves for increasing and decreasing H do not coincide is called *hysteresis*. The arrows show the direction in which H changes on each branch of the curve. *Saturation* takes place beyond points W and Y. The value of M saturates and $B = \mu_0 (M_{\text{saturated}} + H)$. When $H = 0$ there is a *remanent*

[2] Much weaker magnetic moments of the atomic nucleus are considered in Chap. 18.

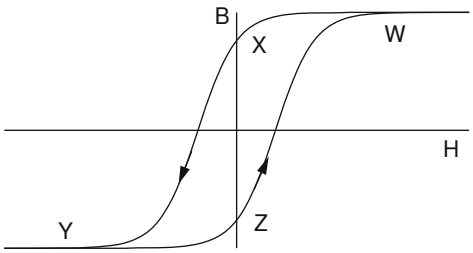

Fig. 8.24 A typical curve of B vs H for a ferromagnetic material. The curve shows hysteresis, and the arrows show the direction of travel around the curve $WXYZ$. Points W and Y show where M saturates. Points X and Z show the remanent magnetic field when $H = 0$

magnetic field (points X and Z). If the temperature of the sample is raised above a critical temperature called the *Curie temperature*, the magnetism is destroyed.

8.8.2 Measuring Magnetic Properties in People

Several kinds of measurements can be based on magnetic effects in materials. A common component of dust inhaled by miners and industrial workers is magnetite, Fe_3O_4, which is ferrimagnetic. By placing the thorax in a fixed magnetic field for a few seconds, the particles can be aligned. The field is turned off and the remanent field measured. The use of *magnetopneumography* in occupational health is described by Stroink (1985). Cohen et al. (1984) have modeled the process by which the particles are magnetized, as well as the relaxation process by which the magnetization disappears after the external field is removed. Relaxation curves are used to estimate intracellular viscosity and the motility of macrophages (scavenger white cells) in the alveoli (Stahlhofen and Moller 1993).

The magnetic susceptibility of blood and myocardium is different from the susceptibility of surrounding lung tissue. An externally applied magnetic field induces a field that changes as the volume of the heart changes. It can be measured externally. The theory and experiments have been described by Wikswo (1980).

Susceptibility measurements can also be used to measure the total iron stores in the body. Normally the body contains 3–4 g of iron. About a quarter of it is stored in the liver. The amount of iron can be elevated from a large number of blood transfusions or in certain rare diseases such as hemochromatosis and hemosiderosis. The liver is an organ whose susceptibility can easily be measured. The susceptibility varies linearly with the amount of iron deposited. Magnetic susceptometry has been used to estimate body iron stores (Nielsen et al. 1995).

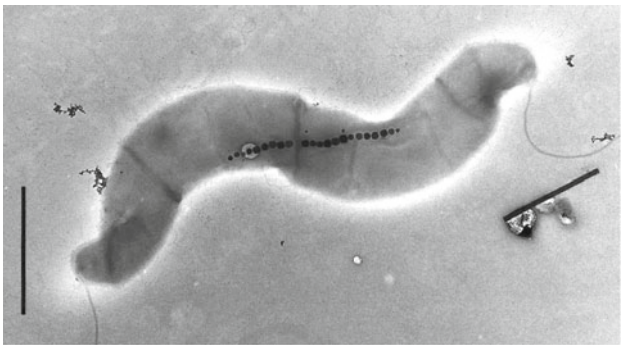

Fig. 8.25 The small black dots are magnetosomes, small particles of magnetite in the magnetotactic bacterium *Aquaspirillum magnetotacticum*. The vertical bar is 1 μm long. The photograph was taken by Y. Gorby and was supplied by N. Blakemore and R. Blakemore, University of New Hampshire.

8.8.3 Magnetic Orientation

Magnetism is used for orientation by several organisms. A history of studies in this area is provided in a very readable book by Mielczarek and McGrayne (2000). Finegold (2012) reviews sensing of static fields. Several species of bacteria contain linear strings of up to 20 particles of magnetite, each about 50 nm on a side encased in a membrane (Frankel et al. 1979; Moskowitz 1995). Over a dozen different bacteria have been identified that synthesize these intracellular, membrane-bound particles or *magnetosomes* (Fig. 8.25). In the laboratory the bacteria align themselves with the local magnetic field. In the problems you will learn that there is sufficient magnetic material in each bacterium to align it with the earth's field just like a compass needle. Because of the tilt of the earth's field, bacteria in the wild can thereby distinguish up from down.

Other bacteria that live in oxygen-poor, sulfide-rich environments contain magnetosomes composed of greigite (Fe_3S_4), rather than magnetite (Fe_3O_4). In aquatic habitats, high concentrations of both kinds of magnetotactic bacteria are usually found near the *oxic–anoxic transition zone* (OATZ). In freshwater environments the OATZ is usually at the sediment–water interface. In marine environments it is displaced up into the water column. Since some bacteria prefer more oxygen and others prefer less, and they both have the same kind of propulsion and orientation mechanism, one wonders why one kind of bacterium is not swimming out of the environment favorable to it. Frankel and Bazylinski (1994) proposed that the magnetic field and the magnetosomes keep the organism aligned with the field, and that they change the direction in which their flagellum rotates to move in the direction that leads them to a more favorable concentration of some desired chemical.

Magnetosomes are found in other species and are likely also to be used for orientation. One species of algae contains about 3000 magnetic particles, each of which is about $40 \times 40 \times 140$ nm (de Araujo et al. 1986). Bees, pigeons, and fish contain magnetic particles. It is more difficult to demonstrate their function, because of the variety of other sensory information available to these animals. For example, homing pigeons with magnets attached to their heads could orient well on sunny days but not on cloudy ones (Walcott et al. 1979). There is evidence that bees orient in a magnetic field (Frankel 1984). The net magnetic moment in the bees is oriented transversely in the body (Gould et al. 1978). In pigeons the magnetic material is located in the dura (the outer covering of the brain) or skull. In all of these cases, the material has been identified as magnetite. In the yellowfin tuna, data are compatible with about 8.5×10^7 magnetic particles, each of which is a single domain of magnetite in the shape of an approximately 50-nm cube (Walker et al. 1984). Recently, Eder et al. (2012) isolated cells from the trout nose and used a rotating magnetic filed to identify cells that are potential magnetite-based magnetoreceptor cells.

Birds may actually have three compasses. Since the magnetic and geographic poles are fairly far apart, migratory birds must correct their magnetic compasses as they fly. The Savannah sparrow is known to have a magnetic compass and a star compass and to take visual cues from the sky at sunset. Able and Able (1995) have shown that adult Savannah sparrows that are subjected to a field pointing in a different direction than the earth's field will at first trust their magnetic compasses, but over a few days they recalibrate their magnetic compasses with their star compasses. An accompanying editorial (Gould 1995) places their work in context. More recently, Cochran et al. (2004) have shown that if migrating thrushes are placed in an eastward-pointing magnetic field at twilight and then released, they fly west instead of south. This strongly suggests that the birds recalibrate their magnetic compass at twilight each day.

The fact that the magnetite particles seem to be about 50 nm on a side is physically significant. Frankel (1984) summarizes arguments that if the particles are smaller than about 35 nm on a side, thermal effects can destroy the alignment of the individual particles. If they are larger than about 76 nm, multiple domains can form within a particle, decreasing the magnetic moment.

8.8.4 Magnetic Nanoparticles

Small single-domain nanoparticles (10–70 nm in diameter) are used to treat cancer (Jordan et al. 1999; Pankhurst et al. 2009). The particles are injected into the body intravenously. Then an oscillating magnetic field is applied. It causes the particles to rotate, heating the surrounding tissue. Cancer cells are particularly sensitive to damage by hyperthermia.

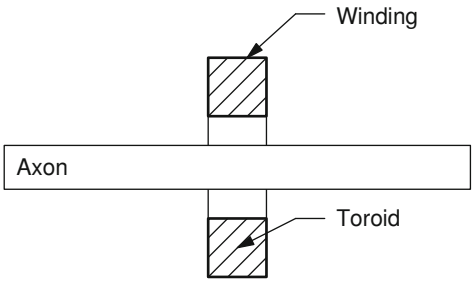

Fig. 8.26 A nerve cell preparation is threaded through the magnetic toroid to measure the magnetic field. The changing magnetic flux in the toroid induces an electromotive force in the winding. Any external current that flows through the hole in the toroid diminishes the magnetic field

Often the surface of the nanoparticle can be coated with antibodies that cause the nanoparticle to be selectively taken up by the tumor, providing more localized heating of the cancer.

8.9 Detection of Weak Magnetic Fields

The detection of weak fields from the body is a technological triumph. The field strength from lung particles is about 10^{-9} T; from the heart it is about 10^{-10} T; from the brain it is 10^{-12} T for spontaneous (α-wave) activity and 10^{-13} T for evoked responses. These signals must be compared to 10^{-4} T for the earth's magnetic field. Noise due to spontaneous changes in the earth's field can be as high as 10^{-7} T. Noise due to power lines, machinery, and the like can be 10^{-5}–10^{-4} T.

If the signal is strong enough, it can be detected with conventional coils and signal-averaging techniques that are described in Chap. 11. Barach et al. (1985) used a small detector through which a single axon was threaded. The detector consisted of a toroidal magnetic core wound with many turns of fine wire (Fig. 8.26). Current passing through the hole in the toroid generated a magnetic field that was concentrated in the ferromagnetic material of the toroid. When the field changed, a measurable voltage was induced in the surrounding coil. This *neuromagnetic current probe* has been used to study many nerve and muscle fibers (Wijesinghe 2010).

The signals from the body are weaker, and their measurement requires higher sensitivity and often special techniques to reduce noise. Hämäläinen et al. (1993) present a detailed discussion of the instrumentation problems. Sensitive detectors are constructed from *superconducting* materials. Some compounds, when cooled below a certain critical temperature, undergo a sudden transition and their electrical resistance falls to zero. A current in a loop of superconducting wire persists for as long as the wire is maintained

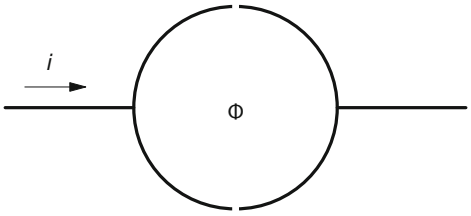

Fig. 8.27 A dc SQUID is shown. The solid lines represent superconducting wires, broken by Josephson junctions at the top and bottom. The total current through both wires depends on Φ, the magnetic flux through the circle

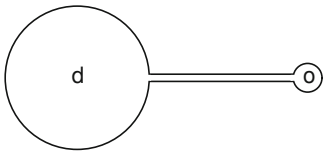

Fig. 8.28 A superconducting loop shaped as shown becomes a flux transporter. Because the total flux in the loop is constant, a change of flux in the detecting loop d is accompanied by an equal and opposite flux change in the output loop o. The diameter of the output loop is matched to the size of the SQUID. Sensitivity is increased because the detecting loop has a larger area

in the superconducting state. The reason there is a superconducting state is a well-understood quantum-mechanical effect that we cannot go into here. It is due to the cooperative motion of many electrons in the superconductor (Eisberg and Resnick 1985, Sect. 14.1; Clarke 1994). The integral $\oint \mathbf{E} \cdot d\mathbf{s}$ around a superconducting ring is zero, which means that $d\Phi/dt$ is zero, and the magnetic flux through a superconducting loop cannot change. If one tries to change the magnetic field with some external source, the current in the superconducting circuit changes so that the flux remains the same.

The detector is called a *superconducting quantum interference device* (*SQUID*). The operation of a SQUID and biological applications are described in the *Scientific American* article by Clarke (1994). Wikswo (1995a) surveys the use of SQUIDs for applications in biomagnetism and nondestructive testing. A technical discussion is also available (Hämäläinen et al. 1993). The dc SQUID requires a superconducting circuit with two branches, each of which contains a very thin nonsuperconducting "weak link" known as a *Josephson junction* (Fig. 8.27). As the magnetic field is changed, these weak links allow the flux in the loop to change. The phase of the quantum mechanical wave function of the collectively moving electrons differs in the two branches by an amount depending on the magnetic flux linked by the circuit. The total current depends on the interference of these two wave functions and is of the form $I = 2I_0 \cos(\pi\Phi/\Phi_0)$, where Φ is the flux through the circuit. The quantity $\Phi_0 = h/2e$, where h is Planck's constant (see Chap. 14) and e is the electron charge, is the *magnetic flux quantum* and has a value equal to 2.068×10^{-15} T m^2. Because interference changes corresponding to a small fraction of this can be measured, the SQUID is very sensitive. The SQUID must be operated at temperatures where it is superconducting. It used to be necessary to keep a SQUID in a liquid-helium bath, which is expensive to operate because of the high evaporation rate of liquid helium. With the advent of high-temperature superconductors, SQUIDS have the potential to operate at liquid-nitrogen temperatures, where the cooling problems are much less severe.

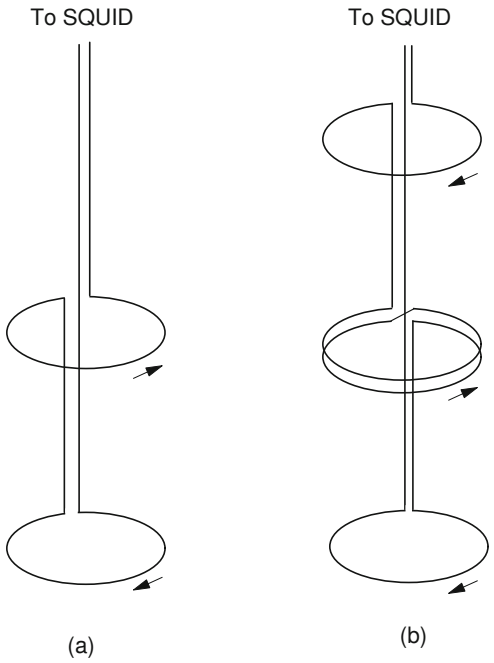

Fig. 8.29 Gradiometers are sensitive to nearby sources of the magnetic field but are much less sensitive to distant sources. **a** A first-order gradiometer. **b** A second-order gradiometer

A typical magnetometer for biomagnetic research contains a *flux transporter*, a superconducting detector coil d a centimeter or so in radius, coupled to a very small multiturn output coil o that matches the size of the SQUID and is placed right next to it. This is shown schematically in Fig. 8.28. The wires between the two loops are close together and have negligible area between them. The total flux, which is constant because the entire circuit is superconducting, is $\Phi = \Phi_d + \Phi_o$. The large area of the detecting coil increases its sensitivity. Any change in the magnetic field at the detector causes an opposite change in the flux and magnetic field at the output coil.

Because ambient natural and artificial background magnetic fields are so high, measurements are often made in special shielded rooms. These can be built of ferromagnetic

materials, or of conductors to take advantage of eddy current attenuation, or they may have active circuits to cancel the background fields. It has proven possible in some cases to eliminate the need for these expensive rooms by using specially designed flux transporters that are less sensitive to distant sources but measure the nearby source with almost the same sensitivity as a single loop. If a distant background source can be represented by a magnetic dipole, the field falls as $1/r^3$. The signal in a magnetometer (Fig. 8.28) would be proportional to this.

Problem 41 shows that the signal from a distant dipole detected by a first-order gradiometer (Fig. 8.29a) is proportional to $1/r^4$ and that the signal in a second order gradiometer (Fig. 8.29b) is proportional to $1/r^5$. Both gradiometers are insensitive to background that does not vary with position. Yet the loop closest to the nearby signal source detects a much stronger signal than the loops that are further away. With modern multi-channel detector systems, one need not use gradiometer coils. Hundreds of coils are used at different locations, and the signals from them are combined to give the same suppression of background from distant sources.

Symbols Used in Chapter 8

Symbol	Use	Units	First used page
a, b	Distance	m	214
e	Elementary charge	C	230
f	Frequency	Hz	215
h	Planck's constant	J s	230
i	Current	A	214
j, $\mathbf{j}$	Current density	A m^{-2}	216
j_d	Displacement current density	A m^{-2}	217
m, $\mathbf{m}$	Magnetic moment	A m^2	214
m	Mass	kg	215
$\mathbf{p}$	Current dipole moment	A m	219
q	Charge	C	213
r, $\mathbf{r}$	Distance	m	215
s, $\mathbf{s}$	Linear displacement	m	213
t	Time	s	217
v, $\mathbf{v}$	Velocity	m s^{-1}	213
v	Electrical potential	V	219
x, y, z	Coordinates	m	217
$\hat{\mathbf{x}}$, $\hat{\mathbf{y}}$, $\hat{\mathbf{z}}$	Unit vectors		219
A	Area	m^2	217
B, $\mathbf{B}$	Magnetic field	T	213
C	Particle concentration	m^{-3}	214
D, $\mathbf{D}$	Electric displacement	C m^{-2}	217
E, $\mathbf{E}$	Electric field	V m^{-1}	214
F, $\mathbf{F}$	Force	N	213
H, $\mathbf{H}$	Magnetic field intensity	A m^{-1}	227
I	Current	A	230
M, $\mathbf{M}$	Magnetization	A m^{-1}	227
M	Mutual inductance	V s A^{-1}	236
R	Position	m	219
S, $\mathbf{S}$	Surface area	m^2	214
T	Period	s	215
V	Volume	m^3	227
ϵ_0	Electrical permittivity of free space	N^{-1} m^{-2} C^2	215
θ	Angle		214
κ	Dielectric constant		217
μ	Magnetic permeability	Ω s m^{-1}	227
μ_0	Magnetic permeability of free space	Ω s m^{-1}	215
σ	Charge per unit area	C m^{-2}	217
σ_i, σ_o	Electrical conductivity	S m^{-1}	219
τ, $\boldsymbol{\tau}$	Torque	N m	214
ϕ	Angle		214
χ_m	Magnetic susceptibility		227
Φ	Magnetic flux	T m^2 or Wb	224
Φ_0	Quantum of magnetic flux	T m^2 or Wb	230

Problems

Section 8.1

Problem 1. An electric dipole consists of charges $\pm q$ separated a distance b. Show that the torque $\boldsymbol{\tau}$ on an electric dipole $\mathbf{p}$ in a steady electric field $\mathbf{E}$ is given by $\boldsymbol{\tau} = \mathbf{p} \times \mathbf{E}$, where $\mathbf{p}$ has magnitude qb, pointing in the direction from $-q$ to $+q$.

Problem 2. Show that the units of $\mathbf{m}$, A m^2 or J T^{-1}, are equivalent.

Problem 3. Show that the units of μ_0, T m A^{-1}, are equivalent to Ω s m^{-1}.

Problem 4. It is possible that the Lorentz force law allows marine sharks, skates, and rays to orient in a magnetic field (Frankel 1984). If a shark can detect an electric field strength of 0.5 μV m^{-1}, how fast would it have to swim through the earth's magnetic field to experience an equivalent force on a charged particle? The earth's field is about 5×10^{-5} T.

Problem 5. The introduction to this section says that magnetism is a consequence of special relativity. Consider the following thought experiment. (a) A line of positive charge lies along the x axis and moves in the positive x direction. Is there a magnetic field present? (b) Change to a frame of reference moving with the charge. In this frame, where the charge is stationary, is there a magnetic field present? So is there really a magnetic field present, or not?

Problem 6. The speed of blood in an artery or vein can be measured using an electromagnetic blood flow meter. A blood vessel of radius R is oriented perpendicular to a magnetic field $\mathbf{B}$. Ions in the blood, which is moving with speed U, experience a Lorentz force. Positive ions move to one side of the vessel and negative ions move to the other side, establishing an electric field E whose force just balances the magnetic force.

(a) Draw a diagram showing the vessel and the directions of **U**, **E**, and **B**.
(b) Find an expression for U in terms of E and B.
(c) The electric field can be approximated as a voltage v across the vessel divided by the width of the vessel. Find an expression for v in terms of U, B and R.
(d) If $B = 0.1\,\mathrm{T}$, $U = 0.01\,\mathrm{m\,s^{-1}}$ and $R = 1\,\mathrm{mm}$, what is v?

Section 8.2

Problem 7. A very long solenoid of radius a has current i in the windings. The windings are closely spaced and there are N turns per meter. What is the magnetic field in the solenoid? (Hint: if the solenoid is very long, the field inside is uniform and the field outside is zero. Use Ampere's law.)
Problem 8. Figure 8.8 uses the Biot Savart law to show that the magnetic field from a spherically symmetric radial distribution of current is zero. Use a simple symmetry argument to obtain the same result.
Problem 9. Show that $d\mathbf{D}/dt$ has the dimensions of current density.
Problem 10. A circular loop of radius a and area S carries current i. The loop is at the origin and lies in the xy plane. Calculate the magnetic field at any point on the z axis using the Biot–Savart law. Show that it is proportional to the magnetic moment of the loop, $|\mathbf{m}| = iS$, and falls off as z^{-3} if $z \gg a$.
Problem 11. Show that a point source of current in an infinite, homogeneous conducting medium discharges at such a rate that the displacement current density everywhere cancels the current density, so that Ampere's law also predicts that the magnetic field is zero.

Section 8.3

Problem 12. Derive Eq. 8.15 from Eq. 8.14.
Problem 13. The current along an axon is $i_i(x) = i_0,\ 0 < x < x_1$ and is zero everywhere else. The axon is in an infinite homogeneous conducting medium.
(a) What is $v_i(x)$?
(b) Find **B** at a point (x_0, y_0).
Problem 14. One can obtain a very different physical picture of the source of a magnetic field using the Biot–Savart law than one gets using Ampere's law, even though the field is the same. A ring of radius a is perpendicular to the x axis and centered at x_0. Current flows along the x axis from $x = 0$ to $x = x_1$. There is a spherically symmetric current in at $x = 0$ and a spherically symmetric current out from x_1. Calculate the magnetic field at a point on the ring using Ampere's law and using the Biot–Savart law. Discuss the difference in interpretation. Your expression for the field should be the same as Problem 13. A more extensive discussion of three different ways the source of the magnetic field can be viewed is given by Barach (1987).

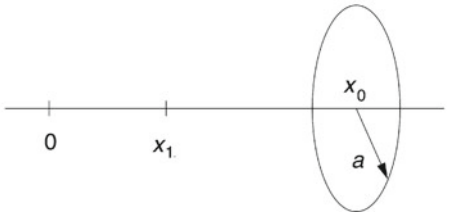

Problem 15. Suppose that $i_i(t)$ is determined by measurement of the magnetic field around an axon. Numerical differentiation of the data gives derivatives of i_i also. Use the arguments of Sect. 6.11 and Problem 6.60 to show that for an action potential traveling without change of shape, one can determine the membrane current density from

$$j_m = \frac{1}{2\pi a u}\frac{\partial i_i}{\partial t} - c_m u r_i i_i .$$

For an application of this technique, see Barach et al. (1985).
Problem 16. Use Ampere's law to calculate the magnetic field produced by a nerve axon.
(a) First, solve Problem 30 of Chap. 7 to obtain the electrical potential inside (V_i) and outside (V_o) an axon. The solution will be in terms of the modified Bessel functions $I_0(kr)$ and $K_0(kr)$, where k is a spatial frequency and r is the radial distance from the center of the axon. Assume the axon has a radius a.
(b) Find the axial component of the current density both inside and outside the axon, $J_{iz} = -\sigma_i \partial V_i/\partial z$ and $J_{oz} = -\sigma_o \partial V_o/\partial z$, where σ_i and σ_o are the intracellular and extracellular conductivities (Eqs. 6.16b and 6.26).
(c) Integrate J_{iz} over the axon cross-section to get the total intracellular current. Then integrate J_{oz} over an annulus from a to radius r, to get the *return current.* You will need the following integrals:

$$\int x I_0(x)dx = x I_1(x)$$

and

$$\int x K_0(x)dx = -x K_1(x).$$

(d) Use Ampere's law (Eq. 8.11) to calculate the magnetic field. Take the line integral of Ampere's law as a closed loop of radius r concentric with the axon ($r > a$). The current enclosed by this loop is simply the sum of the intracellular and return currents calculated in (c).

Section 8.4

Problem 17. Use the same technique as in Chap. 7 to estimate the magnitude of the magnetocardiogram signal.

Problem 18.

(a) Derive Eqs. 8.19 and 8.20.

(b) What effect will y and z components of $\mathbf{p}$ have for measurements taken along an axis with $y = 0$?

Problem 19. Consider a two-dimensional sheet of cardiac tissue represented using the bidomain model (Sect. 7.9.3). The intracellular and extracellular conductivity tensors are given by

$$\widetilde{\sigma_i} = \begin{pmatrix} \sigma_{ixx} & \sigma_{ixy} \\ \sigma_{ixy} & \sigma_{iyy} \end{pmatrix} = \begin{pmatrix} \sigma_{iL}\cos^2\theta + \sigma_{iT}\sin^2\theta & (\sigma_{iL} - \sigma_{iT})\sin\theta\cos\theta \\ (\sigma_{iL} - \sigma_{iT})\sin\theta\cos\theta & \sigma_{iL}\sin^2\theta + \sigma_{iT}\cos^2\theta \end{pmatrix}$$

$$\widetilde{\sigma_o} = \begin{pmatrix} \sigma_{oxx} & \sigma_{oxy} \\ \sigma_{oxy} & \sigma_{oyy} \end{pmatrix} = \begin{pmatrix} \sigma_{oL}\cos^2\theta + \sigma_{oT}\sin^2\theta & (\sigma_{oL} - \sigma_{oT})\sin\theta\cos\theta \\ (\sigma_{oL} - \sigma_{oT})\sin\theta\cos\theta & \sigma_{oL}\sin^2\theta + \sigma_{oT}\cos^2\theta \end{pmatrix}$$

where "L" means parallel to the fibers, "T" means perpendicular to the fibers, and θ is the angle between the fiber direction and the x axis. The intracellular and extracellular current densities are given by $\mathbf{j}_i = \widetilde{\sigma_i} \cdot \mathbf{E} = -\widetilde{\sigma_i} \cdot \nabla v_i$ and $\mathbf{j}_o = -\widetilde{\sigma_o} \cdot \nabla v_o$. Assume that the intracellular and extracellular potentials are given by $v_i = \sigma_{oxx} v_m(x)/(\sigma_{ixx} + \sigma_{oxx})$ and $v_o = -\sigma_{ixx} v_m(x)/(\sigma_{ixx} + \sigma_{oxx})$, where $v_m(x)$ is the transmembrane potential and is a function only of x, corresponding to a plane wave front propagating in the x direction.

(a) Draw a picture showing the 2-D sheet of tissue, the x and y axes, the fiber direction, and the direction of propagation.

(b) Show that $j_x = j_{ix} + j_{ox}$ is identically zero.

(c) Derive an expression for $j_y = j_{iy} + j_{oy}$ in terms of σ_{iL}, σ_{iT}, σ_{oL}, σ_{oT}, θ, and v_m.

(d) Under what conditions is j_y identically zero?

(e) Describe qualitatively the magnetic field produced by a wave front in a sheet of cardiac tissue. For additional features of this model, see Roth and Woods (1999).

Section 8.5

Problem 20. Consider two cylindrical cells of radius 1 μm. One is an axon with an action potential lasting 1 ms and traveling at 1 m s^{-1} with a depolarization amplitude of 100 mV. The other is a dendrite with a postsynaptic potential depolarization of 10 mV. The conductivity within both cells is 1 S m^{-1}.

(a) Compare the magnetic field 5 cm away from the dendrite with depolarization only and the axon with a complete pulse.

(b) If the minimum magnetic field that can be detected is 100×10^{-15} T, how many dendrites must be simultaneously excited to detect the signal?

(c) Pyramidal cells in the cortex are aligned properly to generate this kind of signal. Assume the dendrite is 2 mm long. There are about 50,000 neurons per mm^3 in the cortex, of which 70 % are pyramidal cells. Find the volume of the smallest excited region that could be detected if all the pyramidal cells in the volume simultaneously had a postsynaptic depolarization of 10 mV.

Problem 21. The magnetic field $\mathbf{B}(\mathbf{r})$ produced by a current dipole $\mathbf{p}$ located at $\mathbf{r}_0$ in a spherical conductor is given by Sarvas (1987)

$$\mathbf{B}(\mathbf{r}) = \frac{\mu_0}{4\pi F^2}\left[F\,(\mathbf{p}\times\mathbf{r}_0) - (\mathbf{p}\times\mathbf{r}_0\cdot\mathbf{r})\nabla F\right],$$

where $\mathbf{a} = \mathbf{r} - \mathbf{r}_0$, $a = |\mathbf{a}|$, $r = |\mathbf{r}|$, $F = a(ra + r^2 - \mathbf{r}_0\cdot\mathbf{r})$,

$$\nabla F = \left(\frac{a^2}{r} + \frac{\mathbf{a}\cdot\mathbf{r}}{a} + 2a + 2r\right)\mathbf{r} - \left(a + 2r + \frac{\mathbf{a}\cdot\mathbf{r}}{a}\right)\mathbf{r}_0,$$

and both r and r_0 are measured from the center of the sphere.

(a) Show that if $\mathbf{p}$ is radial, $\mathbf{B} = 0$.

(b) Show that the equation for the radial component of $\mathbf{B}$ reduces to Eq. 8.17. Note that the radius of the sphere does not enter into these equations.

Section 8.6

Problem 22. Consider a rectangular current loop with one corner at $(0, 0, 0)$ and the diagonally opposite corner at $(dx, dy, 0)$, in a changing magnetic field that has components $(0, 0, dB/dt)$. Show that for this configuration the differential form of the Faraday induction law, Eq. 8.22, follows from Eq. 8.21.

Problem 23. Obtain the differential form of Ampere's circuital law, Eq. 8.24, from Eq. 8.13.

Problem 24. The differential form of Ampere's law, Eq. 8.24, provides a relationship between the current density $\mathbf{j}$ and the magnetic field $\mathbf{B}$ that allows you to measure biological current with magnetic resonance imaging (see, for example, Scott et al. (1991)). Suppose you use MRI and find the distribution of magnetic field to be

$$B_x = C(yz^2 - yx^2)$$
$$B_y = C(xz^2 - xy^2)$$
$$B_z = C4xyz$$

where C is a constant with the units of T m^{-3}. Determine the current density. Assume the current varies slowly enough that the displacement current can be neglected.

Problem 25. Write down in differential form (a) the Faraday induction law, (b) Ampere's law including the displacement current term, (c) Gauss's law, and (d) Eq. 8.9. (Ignore the effects of dielectrics or magnetic materials. That is, assume $\mathbf{D} = \varepsilon_0\mathbf{E}$ and $\mathbf{B} = \mu_0\mathbf{H}$.) These four equations together constitute *Maxwell's equations*. Together with the Lorentz force law (Eq. 8.2), Maxwell's equations summarize all of electricity and magnetism.

Problem 26. Consider a square loop of wire in the xy plane that is moving in the positive x direction. There is a static magnetic field with a z component that increases linearly with x. Special relativity implies that the physics should be the same in any inertial frame of reference: that is, the physics should be the same in a reference frame moving with a constant velocity as it is in a frame at rest.

(a) Consider the frame described above, in which the loop moves and the magnetic field is static. Show qualitatively that the Lorentz force on the electrons in the wire induces a current.

(b) Now consider the situation from a frame of reference moving with the loop. Show qualitatively that Faraday induction will induce a current in the wire.

Which "really" caused the current: the Lorentz force or Faraday induction?

Problem 27. Suppose one is measuring the EEG when a time-dependent magnetic field is present (such as during magnetic stimulation). The EEG is measured using a disk electrode of radius $a = 5$ mm and thickness $d = 1$ mm, made of silver with conductivity $\sigma = 63 \times 10^6$ S m^{-1}. The magnetic field is uniform in space, is in a direction perpendicular to the plane of the electrode, and changes from zero to 1 T in 200 μs.

(a) Calculate the electric field and current density in the electrode due to Faraday induction.

(b) The rate of conversion of electrical energy to thermal energy per unit volume (Joule heating) is the product of the current density times the electric field. Calculate the rate of thermal energy production during the time the magnetic field is changing.

(c) Determine the total thermal energy change caused by the change of magnetic field.

(d) The specific heat of silver is 240 J kg^{-1} °C^{-1}, and the density of silver is 10,500 kg m^{-3}. Determine the temperature increase of the electrode due to Joule heating.

The heating of metal electrodes can be a safety hazard during rapid (20 Hz) magnetic stimulation (Roth et al. 1992).

Problem 28. Suppose that during rapid-rate magnetic stimulation, each stimulus pulse causes the temperature of a metal EEG electrode to increase by ΔT (see Problem 27). The hot electrode then cools exponentially with a time constant τ (typically about 45 s). If N stimulation pulses are delivered starting at $t = 0$ with successive pulses separated by a time Δt, then the temperature at the end of the pulse train is $T(N, \Delta t) = \Delta T \sum_{i=0}^{N-1} e^{-i\Delta t/\tau}$. Find a closed form expression for $T(N, \Delta t)$ using the summation formula for the geometric series: $1+x+x^2+\cdots+x^{n-1} = (1-x^n)/(1-x)$. Determine the limiting values of $T(N, \Delta t)$for $N\Delta t \ll \tau$ and $N\Delta t \gg \tau$. (See Roth et al. 1992.)

Problem 29. The concept of *skin depth* plays a role in some biomagnetic applications.

(a) Write Ampere's law (Eq. 8.24) for the case when the displacement current is negligible.

(b) Use Ohm's law (Eq. 6.26) to write the result from (a) in terms of the electric field.

(c) Take the curl of both sides of the equation you found in (b) (Assume the conductivity σ is homogeneous and isotropic).

(d) Use Faraday's law (Eq. 8.22), $\nabla \cdot \mathbf{B} = 0$ (Eq. 8.9), and the vector identity $\nabla \times (\nabla \times \mathbf{B}) = \nabla(\nabla \cdot \mathbf{B}) - \nabla^2\mathbf{B}$ to simplify the result from (c).

(e) Your answer to (d) should be the familiar diffusion equation (Eq. 4.24). Express the diffusion constant D in terms of electric and magnetic parameters.

(f) In Chap. 4, we found that diffusion over a distance L takes a time $T = L^2/2D$. During transcranial magnetic stimulation, $L = 0.1$ m, $\sigma = 0.1$ S $m^{-1}$and $\mu_0 = 4\pi \times 10^{-7}$ T m A^{-1}. How long does the magnetic field take to diffuse into the head? Is this time much longer than or much shorter than the rise time of the magnetic field for the stimulator designed by Barker et al. (1985)?

(g) Solve $T = L^2/2D$ for L, using the expression for D found in (e). Calculate L for $T = 0.1$ ms. Is L much larger than or much smaller than the size of your head? L is closely related to the skin depth defined in electromagnetic theory.

(h) During magnetic resonance imaging (see Chap. 18), an 85-MHz radio-frequency magnetic field is applied to the body. Calculate L using half a period for T. How does L compare to the size of the head? The frequency of the RF field is proportional to the strength of the static magnetic field in an MRI device, and 85 MHz corresponds to 2 T. If the static field is 7 T (common in modern high-field MRI), calculate L. Is it safe to ignore skin depth during high-field MRI?

Section 8.7

Problem 30. Suppose that a magnetic stimulator consists of a single-turn coil of radius $a = 2$ cm. It is desired to have a magnetic field of 2 T on the axis of the coil at a distance $b = 2$ cm away.

(a) Calculate the current required, using symmetry and the Biot–Savart law. (Hint: Use the results of Problem 10.)
(b) Assume that the magnetic field rises from 0 to 2 T in 100 μs. Assume also that the flux through the coil is equal to the field at the center of the coil multiplied by the area of the coil. Calculate the emf induced in the coil.

Problem 31. Assume a sheet of tissue having conductivity σ is placed perpendicular to a uniform, strong, static magnetic field $\mathbf{B}_0$. A weaker but temporally oscillating magnetic field $\mathbf{B}_1(t)$ is parallel to $\mathbf{B}_0$ and is uniform in the region $r < a$, where r is the distance from a line along the direction of $\mathbf{B}_0$.
(a) Derive an expression for the electric field $\mathbf{E}$ induced by the oscillating magnetic field. It will depend on the distance r from the center of the sheet and the rate of change of the magnetic field.
(b) Determine an expression for the current density $\mathbf{j}$ by multiplying the electric field by the conductivity.
(c) The force per unit volume, $\mathbf{F}$, is given by the Lorentz force, $\mathbf{j} \times \mathbf{B}_0$ (ignore the weak $\mathbf{B}_1$). Find an expression for $\mathbf{F}$.
(d) The source of the ultrasonic pressure waves can be expressed as the divergence of the Lorentz Force. Derive an expression for $\nabla \cdot \mathbf{F}$.
(e) Draw a picture showing the directions of $\mathbf{j}$, $\mathbf{B}_0$, and $\mathbf{F}$.

This technique of measuring the ultrasonic signal and determining the conductivity is called *Magnetoacoustic Tomography with Magnetic Induction (MAT-MI)* (Xu and He 2005).

Problem 32.
(a) Rederive the cable equation for the transmembrane potential v, (Eq. 6.55) using one crucial modification: generalize Eq. 6.26 to account for part of the intracellular electric field that arises from Faraday induction and therefore cannot be written as the gradient of a potential,

$$i_i(x) = -\frac{1}{r_i}\left(\frac{dv_i}{dx} + E_{ix}\right).$$

Assume you measure v relative to the resting potential so Eq. 6.53 becomes $j_m = g_m v$, and let the extracellular potential be small so $v_i = v$. Identify the new source term in the cable equation (the *activating function* for magnetic stimulation), analogous to v_r in Eq. 6.55.
(b) Let

$$E_i = E_0 \frac{a^2}{x^2 + a^2}.$$

Calculate the activating function and plot both the electric field and the activating function versus x.
(c) Suppose you stimulate a nerve using this activating function, first with one polarity of the current pulse and then the other. What additional delay in the response of the nerve (as measured by the arrival time of the action potential at the far end) will changing polarity cause because of the extra distance the action potential must travel? Assume $a = 4$ cm and the conduction speed is 60 m s^{-1}.

Section 8.8

Problem 33. Magnetite, Fe_3O_4, has a density of 5.24 g cm^{-3} and a magnetic moment of 3.75×10^{-23} A m^2 per molecule. If a cubic sample 50 nm on a side is completely magnetized, what is the total magnetic moment? What is the magnitude of M?

Problem 34. The magnetic moment of a magnetosome, one of the small particles of magnetite in a bacterium, is about 6.40×10^{-17} A m^2. Assume that the magnetic activity in all the species listed is due to a collection of magnetosomes of this size. The table shows values given in the references cited in the text. The earth's magnetic field is about 5×10^{-5} T. Fill in the remaining entries in the table.

Organism	Number of magnetosomes	Total magnetic moment (A m^2)	mB_{earth}/k_BT
Bacterium	20		
Bee		1.2×10^{-9}	
Pigeon		5.0×10^{-9}	
Tuna	8.5×10^7		

Problem 35. In this problem you will work out the orientation of a bacterium if the entire organism simply aligns like a compass needle in the earth's field of 5×10^{-5} T.
(a) Show that $\boldsymbol{\tau} = \mathbf{m} \times \mathbf{B}$ implies an orientation energy $U = -mB\cos\theta$.
(b) The bacterium has a single flagellum that causes it to swim in the direction of its long axis with speed v_0. The component of its velocity in the direction of the earth's field is $v_x = v_0 \cos\theta$. In the absence of the magnetic torque, the probability that a bacterium is at an angle between θ and $\theta + d\theta$ with the earth's field is proportional to $d\Omega = 2\pi \sin\theta\, d\theta$. With the torque, the probability that a bacterium is at angle with the earth's field is modified by a Boltzmann factor $\exp(-U/k_BT)$. Find the average velocity in the direction of the earth's field. Use $m = 1.28 \times 10^{-15}$ A m^2.

Problem 36. Suppose that the bacterium of Problem 35 is swimming in a tank aligned with the earth's field. An external coil suddenly reverses the direction of the field but leaves the magnitude unchanged. Assume that the bacterium is a sphere of radius a. A torque on a small sphere of radius a in a medium of viscosity η causes the sphere to rotate at a rate $d\theta/dt$, such that $\tau = 8\pi a^3 \eta (d\theta/dt)$. For simplicity, assume that all motion takes place in a plane.

(a) Show that $d\theta/dt = \sin\theta/t_0$, where $t_0 = 8\pi a^3\eta/mB$.
(b) Evaluate t_0 for a bacterium of radius 2 μm in the earth's magnetic field. Use $m = 1.28 \times 10^{-15}$ A m^2
(c) The velocity component perpendicular to the field is $v_y = v_0 \sin\theta$. Show that when the bacterium rotates from angle θ_1 to θ_2 it has moved a distance $y = v_0 t_0(\theta_2 - \theta_1)$.
(d) Show that the time required to change from angle ε to $\pi - \varepsilon$ is $t_0 \ln\left[(1+\cos\varepsilon)/(1-\cos\varepsilon)\right]$.

Problem 37. Magnetic cell sorting is a way to isolate cells of a particular type. Small *superparamagnetic particles* (about 50 nm diameter) are bound to an antibody that attaches specifically to the cell type of interest. (Superparamagnetic means that they behave linearly but have a magnetic susceptibility $\chi_m \gg 1$.) These cells are then placed in a magnetic field gradient, and the resulting force is used to manipulate the cell. What is the force if 100 spherical 50-nm diameter particles are attached to a cell that is in a magnetic field of 1 T with a magnetic field gradient of 10 T m^{-1}?

Section 8.9

Problem 38. The spatial gradient in the earth's field is about 10^{-11} T m^{-1}. How much lateral movement can be tolerated in measuring a magnetoencephalogram of about 10^{-13} T?

Problem 39. Show that the units of $h/2e$ are V s, and that this is also a unit of magnetic flux.

Problem 40. Suppose that a SQUID of area 0.1 cm^2 can resolve a magnetic flux change $\Delta\Phi = 10^{-3}\Phi_0$. What is the corresponding change in B?

Problem 41. The first difference of B is $B(x+a) - B(x)$. What is the second difference? Compare the first and second differences to what is detected by a first-order and second-order gradiometer. Assume that B is constant over the area of each gradiometer loop. Use these results to determine the signal resulting from a distant but unwanted dipole source with a magnetic field that falls as $1/r^3$.

Problem 42. A first-order gradiometer is used to measure the magnetic field at a point $(x_0, 0, z_0)$ from a current dipole described by Eq. 8.18. The gradient is measured at position $z = x_0/\sqrt{2}$. The coils are at x_0 and $x_0 + a$ and are perpendicular to the z axis. Find the net flux in the gradiometer in terms of x_0 and a and the radius b of the coils. Assume B is uniform across each coil.

Problem 43. Figure 8.29a shows a gradiometer for measuring $\partial B_z/\partial z$. Sketch a gradient coil for measuring $\partial B_z/\partial x$.

Problem 44. Consider a nerve threaded through the center of a toroid of magnetic permeability μ, wound with N turns of wire, as shown in Fig. 8.26. The inner radius of the toroid is c, the outer radius is d, and the width is e. Assume a current I flows inside the axon and is uniform along its length.

(a) Calculate the magnetic flux $\Phi = \int \mathbf{B}\cdot d\mathbf{S}$ through the toroid winding caused by the current in the axon.
(b) The magnetic flux divided by the current is called the *mutual inductance*, M, of the axon and coil. Show that the mutual inductance is $M = \mu N e \ln(d/c)/2\pi$.
(c) By the Faraday Induction Law, the electromotive force (EMF) induced in the windings is $EMF = -M(dI/dt)$. Calculate the EMF when $\mu = 10\,000\mu_0$, $N = 100$, $c = 1$ mm, $d = 2$ mm, $e = 1$ mm, and I changes from zero to 1 μA in 1 ms. For additional information about using a toroid to detect currents along an axon, see Gielen et al. (1986).

Problem 45. A coil on a magnetic toroid as in Problem 44 is being used to measure the magnetic field of a nerve axon.
(a) If the axon is suspended in air, with only a thin layer of extracellular fluid clinging to its surface, use Ampere's law to determine the magnetic field, B, recorded by the toroid.
(b) If the axon is immersed in a large conductor such as a saline bath, B is proportional to the sum of the intracellular current plus that fraction of the extracellular current that passes through the toroid (see Problem 14). Suppose that during an experiment an air bubble is trapped between the axon and the inner radius of the toroid. How is the magnetic signal affected by the bubble? See Roth et al. (1985).

Problem 46. When comparing calculated and measured magnetic fields, the calculated field should be integrated over the area of the detector coil to give the magnetic flux through the coil. Assume the detector coil is circular with radius a. The flux can be approximated by

$$\iint \mathbf{B}\cdot d\mathbf{S} \approx \frac{\pi a^2}{3}\sum_{i=1}^{3} B_n\left(r = \frac{a}{\sqrt{2}}, \theta = i\frac{2\pi}{3}\right),$$

where B_n is the component of $\mathbf{B}$ normal to the coil, and r and θ are polar coordinates with the origin at the coil center. Show that this equation is exact up to second order. In other words, show that this equation is exact for magnetic fields given by

$$B_n = c + dx + ey + fx^2 + gxy + hy^2,$$

where c, d, e, f, g, and h are constants, $x = r\cos\theta$, and $y = r\sin\theta$. Higher order formulas for averaging the magnetic field can be found in Roth and Sato (1992).

References

Able KP, Able MA (1995) Interactions in the flexible orientation system of a migratory bird. Nature 375:230–232

Barach JP (1987) The effect of ohmic return currents on biomagnetic fields. J Theor Biol 125:187–191
Barach JP, Roth BJ, Wikswo JP (1985) Magnetic measurements of action currents in a single nerve axon: a core conductor model. IEEE Trans Biomed Eng 32:136–140
Barker AT, Jalinous R, Freeston IL (1985) Non-invasive magnetic stimulation of the human cortex. Lancet 1(8437):1106–1107
Clarke J (1994) SQUIDs. Sci Am (Aug 1994):46–53
Cochran WW, Mouritsen H, Wikelski M (2004) Migrating songbirds recalibrate their magnetic compass daily from twilight cues. Science 304:405–408
Cohen D, Nemoto I, Kaufman L, Arai S (1984) Ferrimagnetic particles in the lung part II: the relaxation process. IEEE Trans Biomed Eng 31:274–285
de Araujo FF, Pires MA, Frankel RB, Bicudo CEM (1986) Magnetite and magnetotaxis in algae. Biophys J 50:375–378
Eder SHK, Cadiou H, Muhamad A, McNaughton PA, Kirschvink JL, Winklhofer M (2012) Magnetic characterization of isolated candidate vertebrate magnetoreceptor cells. PNAS 109:12022–12027
Eisberg R, Resnick R (1985) Quantum physics of atoms, molecules, solids, nuclei and particles, 2nd ed. Wiley, New York
Finegold L (2012) Resource letter BSSMF-1: biological sensing of static magnetic fields. Am J Phys 80:851–861
Frankel RB (1984) Magnetic guidance of organisms. Ann Rev Biophys Bioeng 13:85–103
Frankel RB, Bazylinski DA (1994) Magnetotaxis and magnetic particles in bacteria. Hyperfine Interact 90:135–142
Frankel RB, Blakemore RP, Wolfe RS (1979) Magnetite in freshwater magnetotactic bacteria. Science 203:1355–1356
Freitas C, Mondragon-Llorca H, Pascual-Leone A (2011) Noninvasive brain stimulation in Alzheimer's disease: systematic review and perspectives for the future. Exp Gerontol 46(8):611–627
Gielen FLH, Roth BJ, Wikswo JP Jr (1986) Capabilities of a toroid-amplifier system for magnetic measurement of current in biological tissue. IEEE Trans Biomed Eng 33:910–921
Gielen FLH, Friedman RN, Wikswo JP Jr (1991) In vivo magnetic and electric recordings from nerve bundles and single motor units in mammalian skeletal muscle. Correlations with muscle force. J Gen Physiol 98(5):1043–1061
Gould JL (1995). Constant compass calibration. Nature 375:184
Gould JL, Kirschvink JL, Deffeyes KS (1978) Bees have magnetic remanence. Science 201:1026–1028
Griffiths DJ (2013) Introduction to electrodynamics, 4th ed. Addison-Wesley, Boston
Hallett M, Cohen LG (1989) Magnetism: a new method for stimulation of nerve and brain. JAMA 262:538–541
Hämäläinen M, Hari R, Ilmoniemi RJ, Knuutila J, Lounasmaa OV (1993) Magnetoencephalography—theory, instrumentation, and applications to noninvasive studies of the working human brain. Rev Mod Phys 65(2):413–497
Hari R, Salmelin R (2012) Magnetoencephalography: from SQUIDs to neuroscience. Neuroimage 20th Anniversary Special Edition. Neuroimage 61:386–396
Hosaka H, Cohen D, Cuffin BN, Horacek BM (1976) The effect of torso boundaries on the magnetocardiogram. J Electrocardiol 9:418–425
Ilmoniemi RJ, Ruohonen J, Karhu J (1999) Transcranial magnetic stimulation—A new tool for functional imaging of the brain. Crit Rev Biomed Eng 27(3–5):241–284
Jordan A, Scholz R, Wust P, Fahline H, Roland F (1999) Magnetic fluid hyperthermia (MFH): cancer treatment with AC magnetic field induced ecitation of biocompatible superparamagnetic nanoparticles. J Magn Magn Mater 201:413–419
Mielczarek EV, McGrayne SB (2000) Iron, nature's universal element: why people need iron and animals make magnets. Rutgers U. Press, New Brunswick
Moskowitz BM (1995) Biomineralization of magnetic minerals. Rev Geophys 33(Part 1 Suppl. S):123–128
Nielsen P, Fischer R, Englehardt R, Tondury P, Gabbe EE, Janka GE (1995) Liver iron stores in patients with secondary haemosiderosis under iron chelation therapy with deferoxamine or deferiprone. Brit J Hematol 91:827–833
O'Reardon JP, Solvason HB, Janicak PG, Sampson S, Eisinberg KE, Nahas Z, McDonald WM, Avery D, Fitzgerald PB, Loo C, Demitrack MA, George MS, Sackheim HA (2007) Efficacy and safety of transcranial magnetic stimulation in the acute treatment of major depression. A multisite randomized controlled trial. Biol Psychiatr 62(11):1208–1216
Page CH (1977) Electromotive force, potential difference, and voltage. Am J Phys 45:978–980
Pankhurst QA, Thanh NTK, Jones SK, Dobson J (2009) Progress in applications of magnetic nanoparticles in biomedicine. J Phys D Appl Phys 42:224041
Press WH, Teukolsky SA, Vetterling WT, Flannery BP (1992) Numerical recipes in C: the art of scientific computing, 2nd ed. reprinted with corrections, 1995. Cambridge University Press, New York
Purcell EM, Morin DJ (2013) Electricity and magnetism, 3rd ed. Cambridge University Press, New York
Romer RH (1982) What do "voltmeters" measure?: Faraday's law in a multiply connected region. Am J Phys 50:1089–1093
Rossi S, Hallett M, Rossini PM, Pascual-Leone A, The safety of the TMS Consensus Group (2009) Safety, ethical considerations, and application guidelines for the use of transcranial magnetic stimulation in clinical practice and research. Clin Neurophysiol 120:2008–2039
Roth BJ (1994) Mechanisms for electrical stimulation of excitable tissue. Crit Rev Biomed Eng 22(3/4):253–305
Roth BJ, Sato S (1992) Accurate and efficient formulas for averaging the magnetic field over a circular coil. In Hoke M, Erne SN, Okada TC, Romani GL (eds) Biomagnetism: clinical aspects. Elsevier, Amsterdam
Roth BJ, Wikswo JP Jr (1985) The magnetic field of a single axon: a comparison of theory and experiment. Biophys J 48:93–109
Roth BJ, Woosley JK, Wikswo JP Jr (1985) An experimental and theoretical analysis of the magnetic field of a single axon. In Weinberg H, Stroink G, Katila T (eds) Biomagnetism: applications and theory. Pergamon, New York, pp 78–82
Roth BJ, Pascual-Leone A, Cohen LG, Hallett M (1992) The heating of metal electrodes during rapid-rate magnetic stimulation: a possible safety hazard. Electroencephalogr Clin Neurophysiol 85:116–123
Sarvas J (1987) Basic mathematical and electromagnetic concepts of the biomagnetic inverse problem. Phys Med Biol 32:11–22
Scott GC, Joy MLG, Armstrong RL, Henkelman RM (1991) Measurement of nonuniform current density by magnetic resonance. IEEE Trans Med Imag 10:362–374
Shadowitz A (1975) The electromagnetic field. McGraw-Hill, New York
Stahlhofen W, Moller W (1993) Behaviour of magnetic micro-particles in the human lung. Rad Env Biophys 32(3):221–238
Staton DJ, Friedman RN, Wikswo JP Jr (1993) High resolution SQUID imaging of octupolar currents in anisotropic cardiac tissue. IEEE Trans Appl Superconduct 3(1):1934–1936
Strasburger JF, Cheulkar B, Wakai RT (2008) Magnetocardiography for fetal arrhythmias. Heart Rhythm 5:1073–1076
Stroink G (1985) Magnetic measurements to determine dust loads and clearance rates in industrial workers and miners. Med Biol Eng Comput 23:44–49
Stroink G (1992) Cardiomagnetic imaging. In: Zaret BL et al (eds) Frontiers in cardiovascular imaging. Raven Press, New York, pp 161–177

Stroink G, Blackford B, Brown B, Horacek BM (1981) Aluminum shielded room for biomagnetic measurements. Rev Sci Instrum 52(3):463–468

Swinney KR, Wikswo JP Jr (1980) A calculation of the magnetic field of a nerve action potential. Biophys J 32:719–732

Tan GA, Brauer F, Stroink G, Purcell CJ (1992) The effect of measurement conditions on MCG inverse solutions. IEEE Trans Biomed Eng 39(9):921–927

Trontelj Z, Zorec R, Jazbinsek V, Erne SN (1994) Magnetic detection of a single action potential in *Chara corallina* internodal cells. Biophys J 66:1694–1696

Walcott C, Gould JL, Kirschvink JL (1979) Pigeons have magnets. Science 205:1027–1029

Walker MM, Kirschvink JL, Chang S-BR, Dizon AE (1984) A candidate magnetic sense organ in the yellowfin tuna, *Thunnus albacares*. Science 224:751–753

Wassermann E, Epstein C, Ziemann U (2008) Oxford Handbook of transcranial stimulation. Oxford University Press, Oxford

Wijesinghe R (2010) Magnetic measurements of peripheral nerve function using a neuromagnetic current probe. Exp Biol Med 235:159–169

Wikswo JP Jr (1980) Noninvasive magnetic detection of cardiac mechanical activity: theory. Med Phys 7:297–306

Wikswo JP Jr (1995a) SQUID magnetometers for biomagnetism and nondestructive testing: important questions and initial answers. IEEE Trans Appl Superconduct 5(2):74–120

Wikswo JP Jr (1995b) Tissue anisotropy, the cardiac bidomain, and the virtual cathode effect. In Zipes DP, Jalife J (eds) Cardiac electrophysiology: from cell to bedside, 2nd ed. Saunders, Philadelphia, pp 348–361

Wikswo JP Jr, Gevins A, Williamson SJ (1993) The future of the EEG and MEG. Electroencephalogr Clin Neurophysiol 87:1–9

Woosley JK, Roth BJ, Wikswo JP Jr (1985) The magnetic field of a single axon; A volume conductor model. Math Biosci 76:1–36

Xu Y, He B (2005) Magnetoacoustic tomography with magnetic induction (MAT-MI). Phys Med Biol 50:5175–5187